CHAPTER IV

RESULTS AND DISCUSSION

This chapter was divided into four parts. The first part covered the synthesis and characterization of *N,N,N*-trimethylammonium chitosan chloride (TMC) and *N*-[(2-hydroxyl-3-trimethylammonium)propyl]chitosan chloride (HTACC). The preparations of five types of "leave-on" conditioners and four types of damaged hairs were reported in the second and third parts, respectively. The last part was dedicated to the evaluation of coated hairs with each of the prepared leave-on conditioners in terms of physical and mechanical properties.

4.1 Synthesis and Characterization of Charged Derivatives of Chitosan

4.1.1 *N,N,N*-trimethylammonium chitosan chloride (TMC)

TMC was synthesized by a method based on the methylation of chitosan with iodomethane (CH_3I) in the presence of sodium hydroxide and sodium iodide (Scheme 4-1).

Traditionally, an ion exchange resin, amberlite® IRA402 (Cl^- form), was used to exchange the I^- counter-ion with Cl^-. It was however found that the I^- ion remained in the product, as observed from the precipitation of AgI when the dissolved products were titrated with $AgNO_3$. The amberlite® IRA402 was replaced by NaCl aqueous solution in order to completely replace the I^- by Cl^- in TMC.

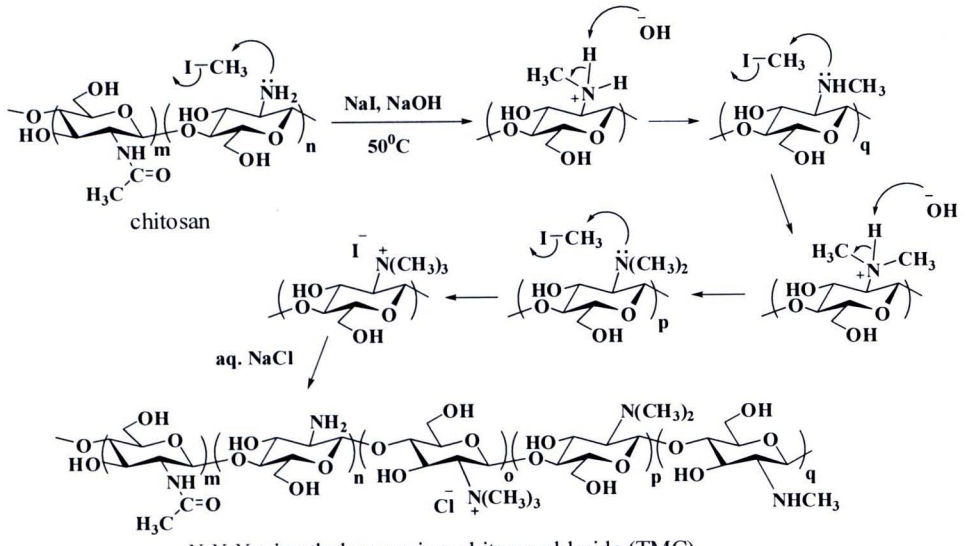

Scheme 4-1 Mechanism of the synthesis of *N,N,N*-trimethylammonium chitosan chloride (TMC) from chitosan by reacting with CH_3I.

Over the past decades, researchers have taken an interest to determine degree of quaternization ($\%DQ$) of TMC by various methods. Sieval *et al.*[2] and Sajomsang *et al.*[54] determine $\%DQ$ from the relative ratio between the signal of $-N^+(CH_3)_3$ and H–1 of the glucosamine ring. Thanou *et al.*[59] determine $\%DQ$ by the ratio between $-N^+(C\underline{H}_3)_3$ and $-COC\underline{H}_3$. The signal of H–2 and H–2′,3,4,5,6,6′ of chitosan could not be used after the methylation process. This is because the signals relates to H–2 as observed at δ 2.95 ppm and H–2′,3,4,5,6,6′ at δ 3.25-4.30 ppm in the chitosan spectrum (Figure 4-1) shift or are overlapped by other signals when TMC is formed. The localization of that peak remains uncertain. However, in this research, the sum of integral signal relates to H–2′,3,4,5,6,6′ at δ 3.25-4.30 ppm in the TMC spectrum was used to determine the $\%DQ$ instead of H–1 signal to compare with $-N^+(CH_3)_3$ signals. It was found that H–1 shifted and was overlapped by solvent signal, H–2 was overlapped by the signal of $-N^+(CH_3)_3$, and the signal of $-COCH_3$ was interfered by trace acetic acid solvent. Nevertheless, the relative ratio between the signal of H–1, H–2, H–2′,3,4,5,6,6′, H–2,2′,3,4,5,6,6′ or $-COCH_3$ and the signal of $-N^+(CH_3)_3$ were determined as shown in Appendix A. The standard derivative of the relative ratio between the signal of H–2′,3,4,5,6,6′ and $-N^+(CH_3)_3$ is the smallest value and $\%DS\,(total)$ is closed to 100.

The ^{1}H NMR spectra of the synthesized TMCs is depicted in Figure 4-1. It is similar to the spectrum reported by Sieval *et al.*[2] The *%DQ* of TMCs were determined from the relative ratios between the signal at 3.10 ppm assigned to three methyl groups of quaternary ammonium group and the sum of integral signal of H–2′,3,4,5,6,6′ of chitosan (δ 3.25-4.30 ppm) analyzed by ^{1}H NMR (Figure 4-1). Moreover, $\%DS_{N(CH_3)_2}$, $\%DS_{NHCH_3}$, *%DS (total)*, *%DOM-3*, and *%DOM-6* are *N,N*-dimethylation, *N*-methylation, a total degree of *N*-methylation, *O*-methylation at 3-hydroxyl, and *O*-methylation at 6-hydroxyl positions of GlcN of chitosan were determined from ^{1}H NMR. The positions of those signals in the TMC spectra are shown in Figure 4-1.

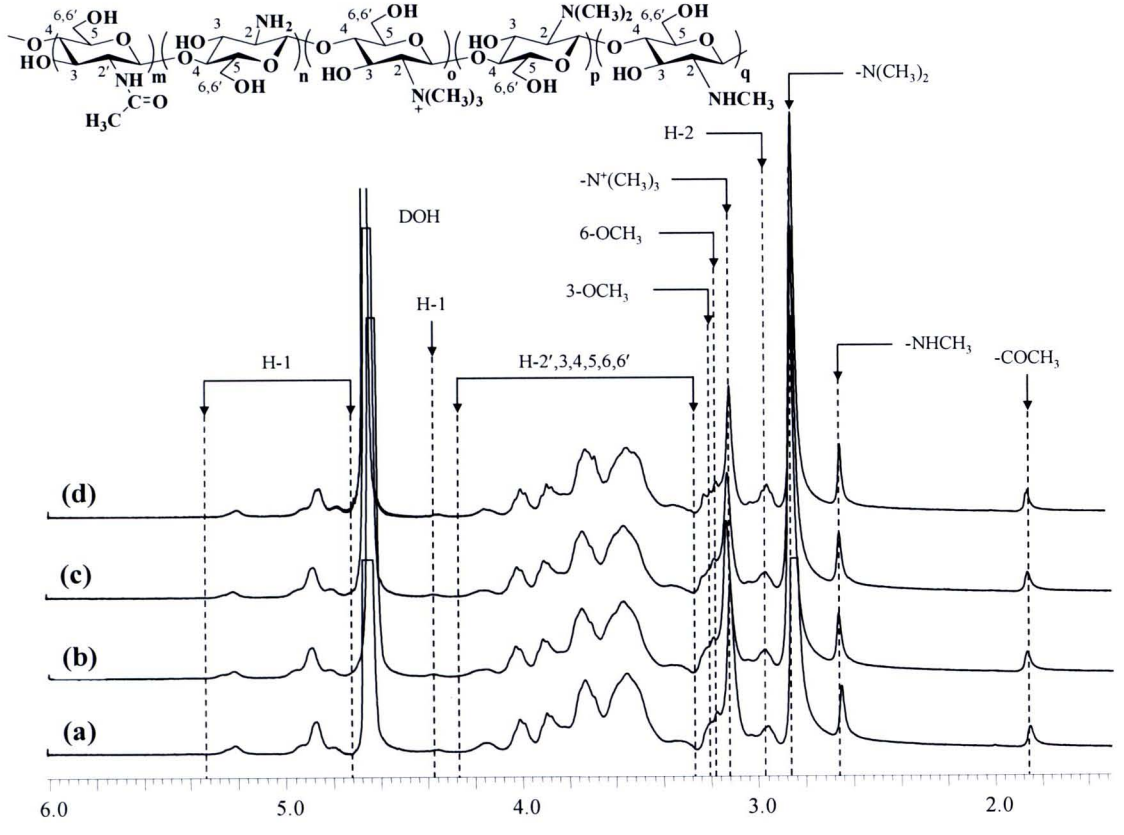

Figure 4-1 ^{1}H NMR spectra of synthesized TMCs using (a) 4, (b) 5, (c) 6, and (d) 12 equivalents of CH_3I in comparison with the number of NH_2 in chitosan (solvent: D_2O/TFA, 25°C).

In this study, the resulting *%DQ's* of TMC or the composition of trimethylated amino groups of chitosan after methylation with iodomethane (4, 5, 6, and 12 eq) are ranged from 17 to 22%, which are almost independent of the iodomethane equivalent. Moreover, replacing NMP solvent by DMF:H_2O (1:1) or H_2O could increase

methylating efficiency of iodomethane on the chitosan for upto $15\%DQ$. Based on the lowest chemical costs and toxicity, TMC synthesis by using 4 eq of CH_3I was therefore suggested as an optimal preparation method of TMC for this study.

Table 4-1 *%DQ* as determined by ^{1}H NMR of quaternary ammonium group on chitosan after reacting with iodomethane at 50°C in NMP, DMF:H_2O (1:1) or H_2O as the reaction solvent.

Equivalent of CH_3I	Solvent	*%DQ* (1)	$\%DS_{N(CH_3)_2}$ (2)	$\%DS_{NHCH_3}$ (3)	*%DS (total)* (1)+(2)+(3)	*%DOM-3*	*%DOM-6*	%Recovery
4	NMP	21.7 ± 0.1	71.6 ± 5.7	10.2 ± 3.4	103.5 ± 9.2	8.7 ± 2.3	24.1 ± 3.6	82.0
5	NMP	21.1 ± 0.4	70.3 ± 3.1	24.6 ± 1.4	116.0 ± 2.4	13.5 ± 1.3	19.3 ± 1.1	95.4
6	NMP	17.8 ± 0.1	70.1 ± 0.2	14.0 ± 8.7	101.9 ± 8.6	9.1 ± 5.5	24.4 ± 4.9	80.3
12	NMP	17.1 ± 0.4	62.8 ± 0.7	15.4 ± 5.3	95.3 ± 6.0	8.4 ± 3.3	22.2 ± 1.8	64.7
4[a]+12[b]	NMP, DMF:H_2O (1:1)	30.8 ± 1.1	90.2 ± 0.8	8.5 ± 5.5	129.6 ± 3.7	7.8 ± 1.4	26.7 ± 5.0	83.4
4[a]+12[c]	NMP, H_2O	34.5 ± 1.8	88.7 ± 2.6	4.7 ± 0.6	128.0 ± 3.9	14.5 ± 1.0	40.4 ± 1.4	69.7

%DQ is degree of quaternization; $\%DS_{N(CH_3)_2}$ is *N,N*-dimethylation; $\%DS_{NHCH_3}$ is *N*-methylation; *%DS (total)* is total degree of *N*-methylation; *%DOM* is degree of *O*-methylation at 3-O and 6-O at 3-hydroxyl and 6-hydroxyl positions of GlcN of chitosan, respectively; %Recovery is weight of product (g)/weight of starting reactants (g)×100

[a]Methylating with 4 eq of iodomethane in NMP, [b]Methylating with 12 eq of iodomethane in DMF:H_2O (1:1), [c]Methylating with 12 eq of iodomethane in H_2O

4.1.2 *N*-[(2-hydroxyl-3-trimethylammonium)propyl]chitosan chloride (HTACC)

HTACCs were synthesized by epoxide ring opening of glycidyltrimethyl ammonium chloride (GTMAC) (Scheme 4-2) by the amino groups of chitosan under acidic condition. GTMAC mainly reacts with amino groups of chitosan under acidic condition but preferably reacts with hydroxyl groups under neutral and alkaline conditions. The acidic condition causes protonation at the oxygen atom and makes the epoxy ring of GTMAC more reactive towards the NH_2 groups of chitosan.

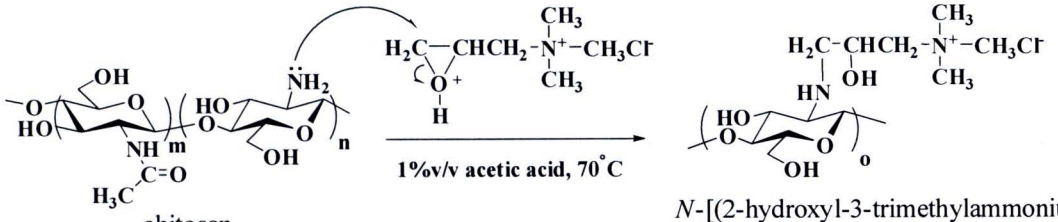

Scheme 4-2 Mechanism of the synthesis of *N*-[(2-hydroxyl-3-trimethylammonium) propyl]chitosan chloride (HTACC).

Figure 4-2 illustrates ^{1}H NMR spectra of the synthesized HTACCs. All signals found in this work match the result reported by Cho *et al.*[55] and Lim *et al.*[56] Signals corresponding to the protons of (a) $-NHC\underline{H}_2-$, (b) $-C\underline{H}(OH)-$, and (c) $-C\underline{H}_2-$ appeared at δ 2.88, 4.44 and 3.32 ppm, respectively. A strong peak at δ 3.05 ppm indicates the presence quaternary ammonium group $-N^+(C\underline{H}_3)_3$ in the obtained product, and is used in $\%DQ$ calculation (equation 3.1).

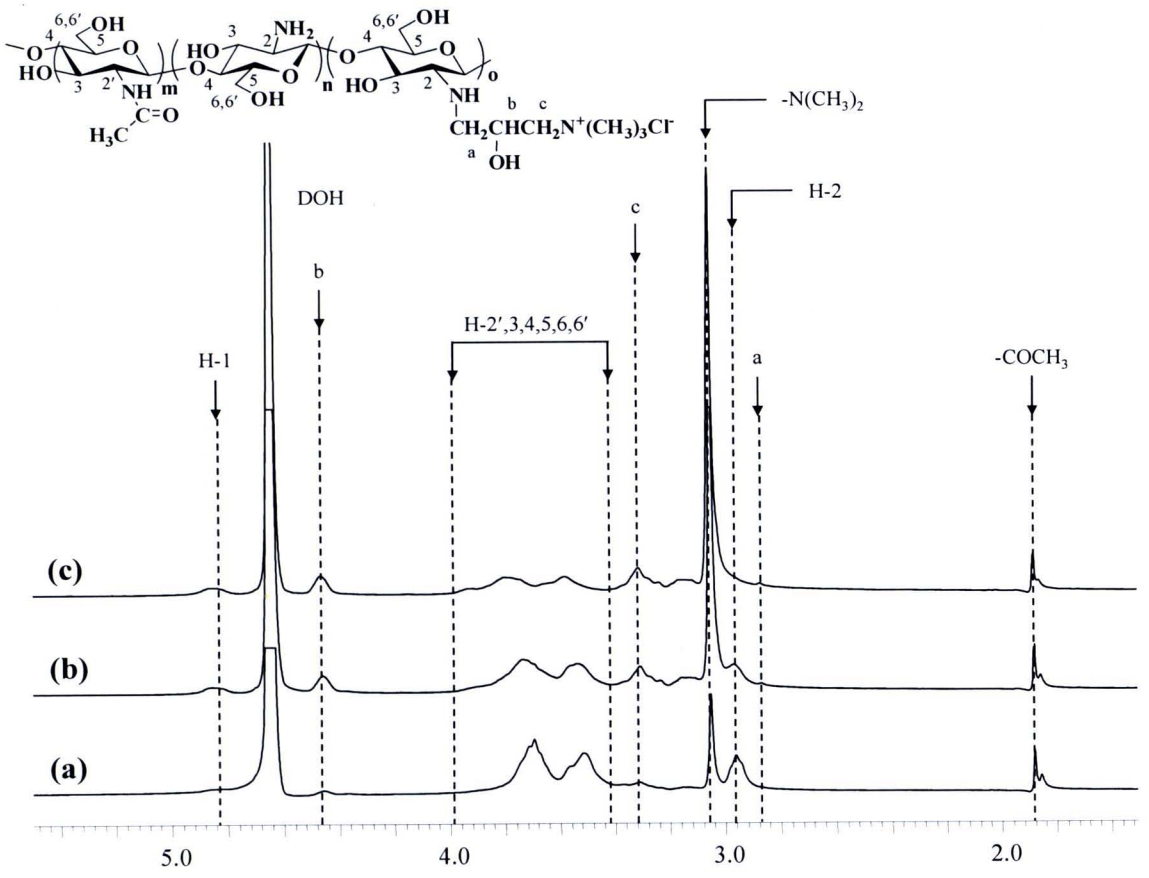

Figure 4-2 ^{1}H NMR spectra of synthesized HTACCs using (a) 2, (b) 4, and (c) 6 equivalents of GTMAC in comparison with the number of NH_2 in chitosan (solvent: D_2O/TFA, 25°C).

In this study, *%DQ* of HTACC was determined from the relative ratio between the area of H signal from the trimethyl ammonium group of grafted GTMAC at δ 3.05 ppm and the sum of integral signal of H–2′,3,4,5,6,6′ (δ 3.40-4.00 ppm) from all pyranose repeat units. From Table 4-2, the *%DQ* on chitosan was increased from 24 to 139 when the GTMAC equivalent used in the synthesis and the reaction time were increased from 2 to 6 and from 2 to 24 h, respectively. It was however found that increase of mole equivalent resulted in more drastic increase of *%DQ* than an increase of reaction time. Moreover, the *%DQ* of HTACC was more than 100% when 6 eq of GTMAC was used. It was possibly because of an error from peak integration caused by signal overlapping between the signal of $-N^{+}(C\underline{H}_3)_3$ and H–2 [Figure 4-2(c)].

Based on chemical costs and toxicity, the synthesis scheme that required the lowest amount of GTMAC but yielded a soluble derivative was preferred. Therefore,

the amount of GTMAC was set at be 2 eq for preparing HTACC for use in leave-on conditioner.

Table 4-2 *%DQ* as determined by ^{1}H NMR on chitosan after reacting with GTMAC at 70°C in 1%v/v acetic acid at different reaction time.

Equivalent of GTMAC	Time (h)	*%DQ*	%Recovery
2	24	23.8 ± 0.3	53.9
4	2	37.8 ± 0.1	62.5
4	4	62.2 ± 0.4	83.7
4	8	77.1 ± 0.7	93.6
4	12	84.6 ± 1.5	71.5
4	24	84.4 ± 0.6	121.3
6	24	139.4 ± 2.7	126.9

%DQ is degree of quaternization.; %Recovery is weight of product (g)/weight of starting reactants (g)×100

Besides ^{1}H NMR, the *%DQ* of TMCs and HTACCs were also determined by conductivity titration method. This method was used to analyze the amount of chloride ion at the lowest conductivity found in the TMC or HTACC solution. The *%DQ* was calculated as follows:

$$\%DQ_{(TMC)} = \frac{1.7\times10^{-5}\times V_{AgNO_3}}{\left(\frac{W_w-(1.7\times10^{-5}\times V_{AgNO_3}\times m_{CH_3Cl})}{(m_G\times DD)+m_{AG}(1-DD)}\right)\times DD}\times 100 \quad (4.1)$$

$$\%DQ_{(HTACC)} = \frac{1.7\times10^{-5}\times V_{AgNO_3}}{\left(\frac{W_w-(1.7\times10^{-5}\times V_{AgNO_3}\times m_{GTMAC})}{(m_G\times DD)+m_{AG}(1-DD)}\right)\times DD}\times 100 \quad (4.2)$$

Table 4-3 $\%DQ$ of $TMC_{CH_3I\ 6eq}$ and $HTACC_{GTMAC\ 4eq\_24hr}$, determined by ^1H NMR spectroscopy and conductivity titration method.

Sample	$\%DQ$		
	^1H NMR	Conductivity titration	
		pH = 5.0	pH = 7.0
$TMC_{CH_3I\ 6eq}$	17.8 ± 0.1	101.7	69.4
$HTACC_{GTMAC\ 4eq\_24hr}$	84.4 ± 0.6	113.9	54.1

As a result, the $\%DQ's$ of TMC and HTACC at pH 5.0 are more than the $\%DQ$ at pH 7.0. This is because at pH 5 the $-NH_2$ group is protonated, resulting in more Cl^- than expected. From the results, $\%DQ$ obtained from the conductivity titration method was not used as the tool to determine $\%DQ$ because it was too sensitive to acidic pH, and had a high tendency to produce unreliable results.

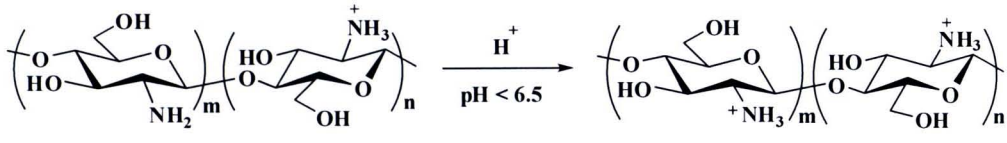

Scheme 4-3 Protonation of amino groups of chitosan at p*K*a.

According to FTIR spectra, the IR spectrum was consistent with the reported spectra.[3,52] The formation of TMC and HTACC was verified by the decrement of the N–H bending peak signal at 1597 cm^{-1} of the amino groups of chitosan and the appearance of the C–N stretching peak of the methyl groups in quaternary ammonium groups at 1480 cm^{-1} (Figure 4-3). Besides, the characteristic peaks of C–O stretching of primary and second alcohol at 1040 and 1080 cm^{-1} are also present in chitosan, TMC, and HTACC.

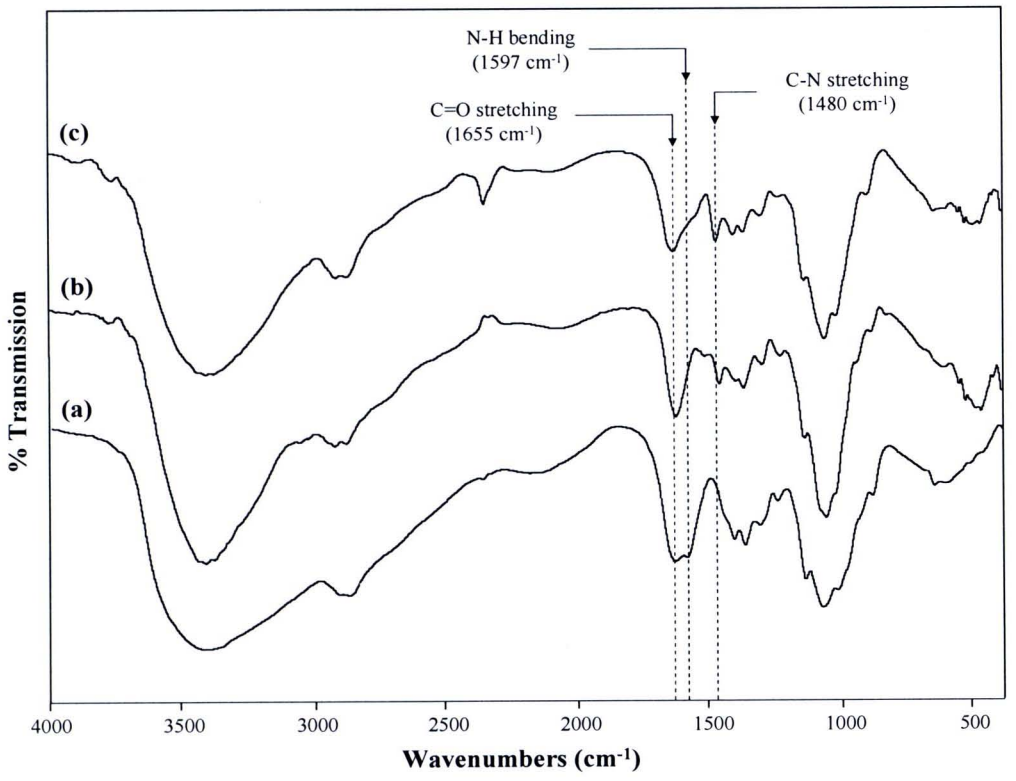

Figure 4-3 FTIR spectra of (a) chitosan, (b) TMC, and (c) HTACC.

4.1.3 Solubility tests of the charged derivatives of chitosan

The solubility test was performed according to a method of Sashiwa *et al.*[58] A solid sample of charged derivatives of chitosan (100 mg) was mixed in water (20 mL). The pH of the solution was adjusted with 0.5%w/v aqueous HCl and NaOH. As illustrated in Table 4-4, chitosan dissolves in acidic region pH below 6.5. The solubility of chitosan in the acidic region is ascribed to the protonation of amino group (from $-NH_2$ to $-NH_3^+$). The synthesized TMC with 17-22$\%DQ$ is unexpectedly insoluble in basic solution at pH above 6.5. It was possible that $\%DQ$ of TMC was too low to dissolve in neutral and basic aqueous media. In addition, the methylation at –OH group, as evidenced by the NMR result (Figure 4-1), can reduce H–bonding site on the polymer structure. On the contrary, HTACC with 24-139 $\%DQ$ is soluble over the entire pH range. However, 2 eq of GTMAC cannot be soluble at pH above 13 due to low DQ (24%).

Table 4-4 *%DQ* and solubility test in water of various pHs[a] of chitosan, TMCs, and HTACCs.

Sample	%DQ	Solubility[b] pH: 1 2 3 4 5 6 7 8 9 10 11 12 13 14
chitosan	-	6.50
TMC $_{CH_3I\ 4eq}$	22	6.62
TMC $_{CH_3I\ 5eq}$	21	6.73
TMC $_{CH_3I\ 6eq}$	18	6.55
TMC $_{CH_3I\ 12eq}$	17	7.03
HTACC $_{GTMAC\ 2eq}$	24	12.93
HTACC $_{GTMAC\ 4eq}$	84	
HTACC $_{GTMAC\ 6eq}$	139	

[a]Solid sample (100 mg) was dispersed in H_2O (20 mL). The pH of the solution was adjusted with 0.5%w/v aqueous HCl and NaOH.

[b]White bar = soluble, black bar = insoluble.

4.1.4 *In vitro* cytotoxicity of chitosan and its charged derivatives

To the best of our knowledge, there are few reports[60,61] explaining in detail the biological response of human keratinocyte cells line and the HaCaT cells line against chitosan and positively charged derivatives. Therefore, the cytotoxicity of chitosan and positive-charged chitosan on the HaCaT cells was investigated. This test is in fact crucial since the polymers are to be used in a product that directly contacts human skin. All tests were performed in pH 6.0 medium, the same pH as in the leave-on conditioner.

The result of MTT test was displayed in Figure 4-4. Cell viabilities of chitosan, TMCs and HTACCs having different *DQs* were investigated as a function of concentration. The IC_{50} values or the half-maximum inhibitory concentrations, which represented concentration of the polymers resulting in 50% inhibition of cell growth, were calculated from a logarithmic regression which obtained from plotted graph of the concentration (x axis) and the cell viability (y axis) as shown in Appendix B. Log_{10} scale is frequently used when concentration values are a serial dilution.

As a result, chitosan in acidic media inhibited cell viability due to the fact that its amino group ($-NH_2$) was converted to an ammonium ion ($-NH_3^+$) that electrostatically interacted with the negatively charged cell membrane. All derivatized polymers exhibited dose-dependent cytotoxicity response, that increased with the $\%DQ$. Both chitosan derivatives in acidic media also inhibited cell viability due to the ammonium ion ($-NH_3^+$) and the quaternized group. IC_{50} of TMC with 18-22$\%DQ$ indicated dose-dependent cytotoxicity in the concentration range of 14.1, 38.6, 1725.9 μg/mL as shown in Table 4-5. The reason for the high toxicity of TMC having 21 and 18$\%DQ$ is unclear but it may happen from the remaining of the material which was used in the synthesis. HTACC with 24-139$\%DQ$ also indicated dose-dependent cytotoxicity in the concentration range of 174.2, 181.9, >1000 μg/mL as shown in Table 4-5. Increasing the equivalent of GTMAC resulted in the HTACC with increased toxicity to the HaCaT cells line. The cytotoxicity was not much increased when using 4 to 6 equivalents of GTMAC. According to the cytotoxicity results, HTACC is less toxic than TMC when compared between samples with similar $DQ's$ as shown in Figure 4-4(B) and (C). The mechanism by which chitosan and its derivative interacts with HaCaT cells line is unclear. It may interact with growth factors in the serum or metal ions (e.g. calcium), reducing the availability of these to the cells.[60] Nevertheless, there are currently very few detailed reports on the effect of chitosan and its derivatives on HaCaT cells line or primary human keratinocytes.

From the cytotoxicity results obtained, it can be concluded that 4 eq of iodomethane per amino groups of chitosan ($TMC_{CH_3I\ 4eq}$) and 2 eq of GTMAC per amino groups of chitosan ($HTACC_{GTMAC\ 2eq}$) are the materials of choice in preparing the conditioners, since they both showed the least toxic effect against the HaCaT cells line.

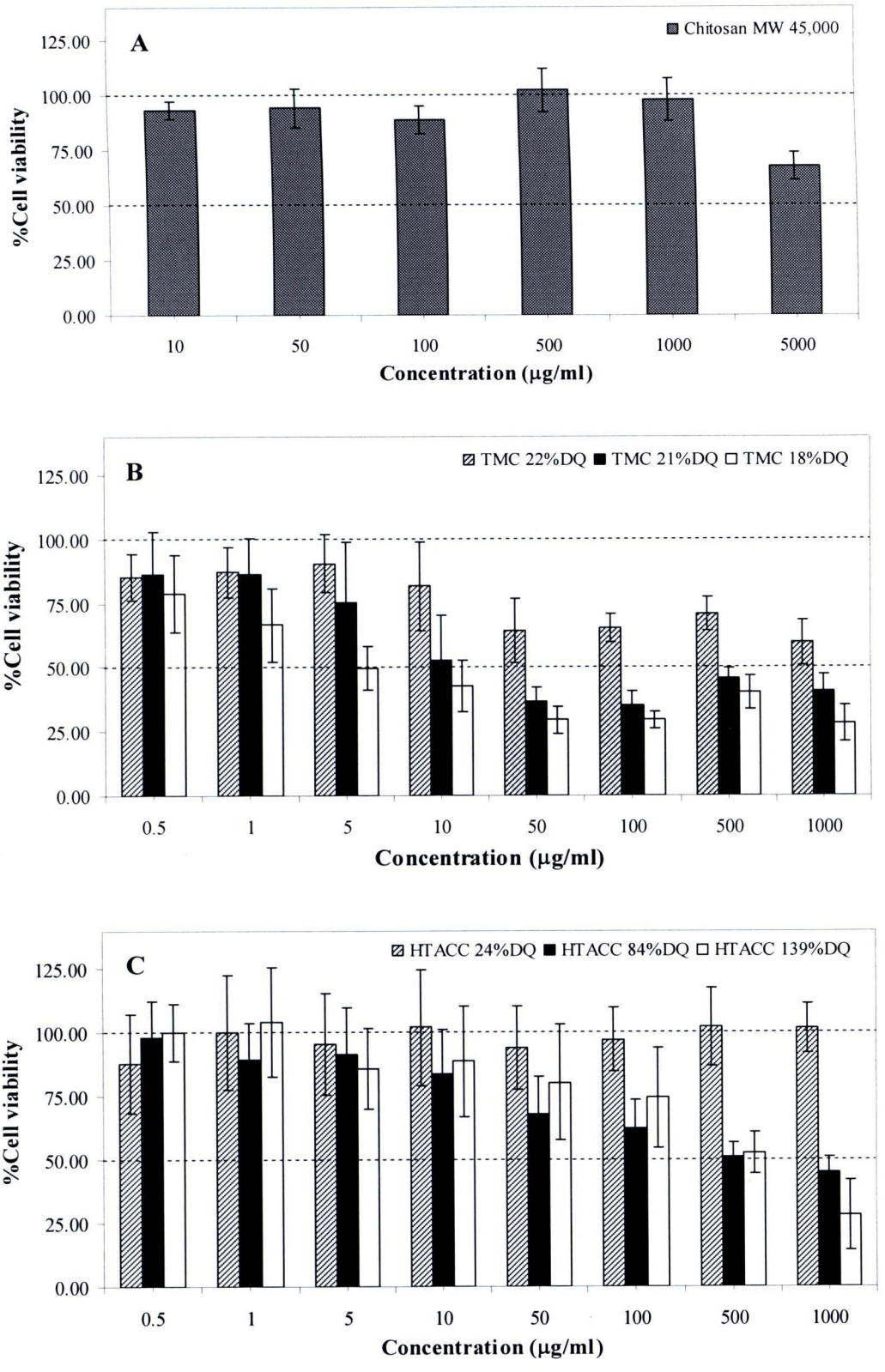

Figure 4-4 *In vitro* cytotoxicity of (A) chitosan MW 45,000, (B) TMCs, and (C) HTACCs on HaCaT cells line as determined by the MTT assay at pH 6.0. The cell viability compared with cell culture medium without polymer. The data shown were averaged from 5 data sets for chitosan and 12 data sets for the chitosan derivatives.

Table 4-5 IC_{50} (μg/mL) of chitosan and its charged derivatives on HaCaT cells line as determined by the MTT assay at pH 6.0.

Sample treatment	*%DD*	*%DQ*	IC_{50} (μg/mL)
Chitosan	85	–	>5000[a]
$TMC_{CH_3I\ 4eq}$	–	22	1725.9
$TMC_{CH_3I\ 5eq}$	–	21	38.6
$TMC_{CH_3I\ 6eq}$	–	18	14.1
$HTACC_{GTMAC\ 2eq}$	–	24	>1000[a]
$HTACC_{GTMAC\ 4eq}$	–	84	181.9
$HTACC_{GTMAC\ 6eq}$	–	139	174.2

[a] The IC_{50} value could not certainly calculated due to the log (x) value is negative.

Additionally, *in vitro* cytotoxicity tests will be more convincing when performed with cells that are homologous with the cell in hair skin. In accordance, cell lines for use in cytotoxicity concerning the skin would be human dermal fibroblasts and human epidermal keratinocytes, as they take an active part in the immune response, inflammatory processes, and wound healing.[62] The evaluation of the cytotoxicity of chitosan and charged derivatives is based on several factors such as passage numbers of cell cultures, growth behavior of cell culture after direct or indirect contact with the materials, growth factors in the serum, and the different environment of *in vitro* and *in vivo*. Another suggestion is the cytotoxicity test should be also performed using the whole leave-on conditioner in order to closely simulate real usage.

4.2 Positively-Charged Chitosan Contents in Leave-On Conditioners

In general, the amount of positively charged macromolecules mixed in the leave-on conditioner is varied upon the type of macromolecules. These positively charged molecules have been used to help control viscosity and attraction to negatively charged hair surface. In this study, chitosan, TMC, or HTACC was used to replace a polyquaternium-10 (commercial ingredient) in the conditioner. The amount and *%DQ* of the chitosan and its charged derivatives must be at optimum level in order to achieve

good homogeneity and viscosity of the prepared conditioner. The investigation therefore focused on five important factors i.e. chemical costs, solubility, cytotoxicity on HaCaT cells line, the ability to attach to human hair, and homogeneity and viscosity of the prepared leave-on conditioners.

As discussed in section 4.1, TMC (*22%DQ*) and HTACC (*24%DQ*) were chosen for the conditioner, because these had the lowest cost and toxicity. Solubility of TMCs and HTACCs did not influence on the selection due to the fact that the pH value of the leave-on conditioner was between 4.5 to 5.5, in which TMCs and HTACCs were in the soluble forms.

4.2.1 Hair coating behavior

Black virgin hairs from an Asian thirty two-year old female used in this study were supported by Life Science Cosmetics Research Center Co., Ltd. Prior to the coating experiment, the hair samples were shampoo-washed and rinsed with DI water three times. Afterward, they were blown dry with cold air and left at room temperature overnight.

Surface characterization of virgin hair was done by ATR FT-IR microspectroscopy with a slide-on Ge μIRE. This novel method was nondestructive. The small contact area of μIRE was less than 100×100 μm^2 which was suitable for the hair samples. The analysis time was rather short but the results were accurate and reliable.

The ATR FT-IR spectrum acquired by Ge μIRE of the virgin hair was shown in Figure 4-5. The observed spectrum shows a broad band at 3277 cm^{-1} attributed to O–H stretching of water together with N–H stretching vibration. The predominant absorption bands at 1641, 1532 and 1234 cm^{-1} are related to amide I, amide II and amide III vibrations, respectively. The absorption bands at 2957-2851 cm^{-1} and 1454, 1406 cm^{-1} are the C–H stretching and C–H deformation vibration, respectively. The IR peak assignments are summarized in Table 4-6.

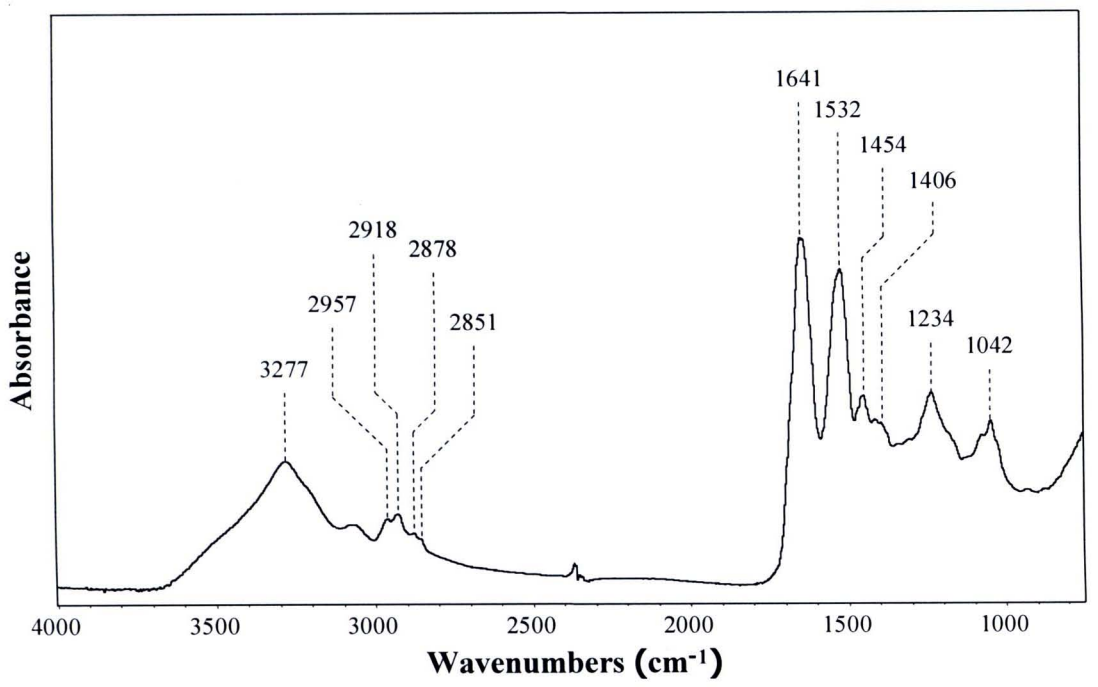

Figure 4-5 ATR FT-IR spectrum of virgin hair.

Table 4-6 Peak assignment of virgin hair used in this study.

Wavenumbers (cm^{-1})		Assignments
Literature[38]	Current work	
3295	3277	asymmetric N–H stretching
2960	2957	asymmetric C–H stretching of CH_3
2926	2918	asymmetric C–H stretching of CH_2
2875	2878	symmetric C–H stretching of CH_3
2851	2851	symmetric C–H stretching of CH_2
1670-1643	1641	Amide I C=O stretching and a small contribution from N–H bending (scissoring)
1548-1517	1532	Amide II C–N stretching plus N–H bending (wagging)
1453	1454	C–H bending (scissoring) of CH_2
1397	1406	C–H bending (wagging) of CH_3
1311-1239	1234	Amide III N–H bending (twisting) plus C–N stretching and contribution from O=C–N bending
1040	1042	S=O

The ATR-FTIR spectra of coated hair sample are shown in Figures 4-6 to 4-8. Apparently, chitosan, TMC (22%*DQ*), and HTACC (24%*DQ*) were detected on the coated unaltered hair samples as demonstrated by the presence of C–O stretching signals of primary and secondary alcohol at 1040 and 1080 cm^{-1} of chitosan structure. For TMC and HTACC, these signals remarkably increased when the concentration (1-3%w/w) of coating solution increased [Figures 4-7(b-d) and 4-8(b-d)]. Interestingly, the intensity increase of C–O signal of chitosan-coated hair was not as high as those of TMC-, HTACC-coated hairs. This probably suggests that the amount of chitosan coated on the hair strand is less than that of the two derivatives.

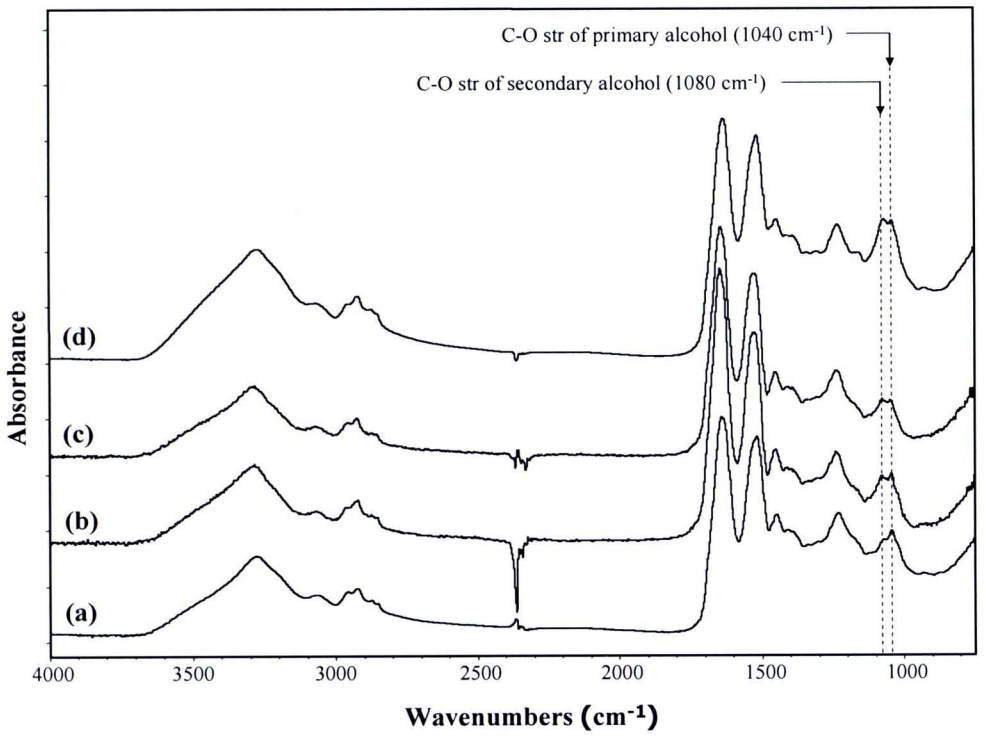

Figure 4-6 ATR FT-IR spectra of (a) virgin hair, (b) coated hair with 1%w/w chitosan solution, (c) coated hair with 2%w/w chitosan solution, and (d) coated hair with 3%w/w chitosan solution.

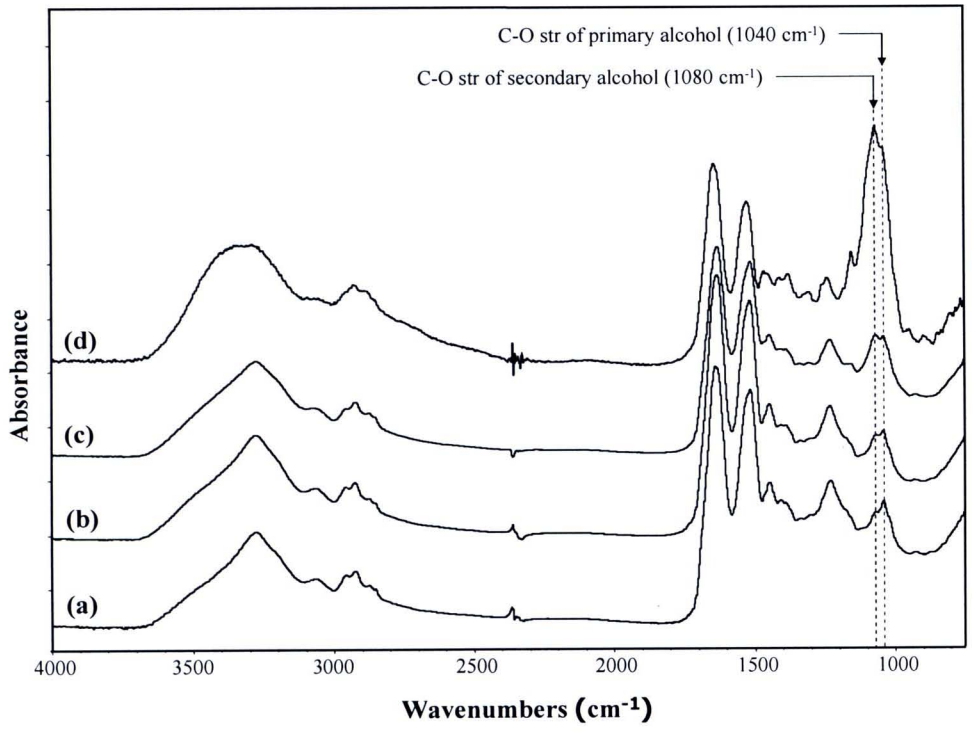

Figure 4-7 ATR FT-IR spectra of (a) virgin hair, (b) coated hair with 1%w/w TMC (22%*DQ*) solution, (c) coated hair with 2%w/w TMC (22%*DQ*) solution, and (d) coated hair with 3%w/w TMC (22%*DQ*) solution.

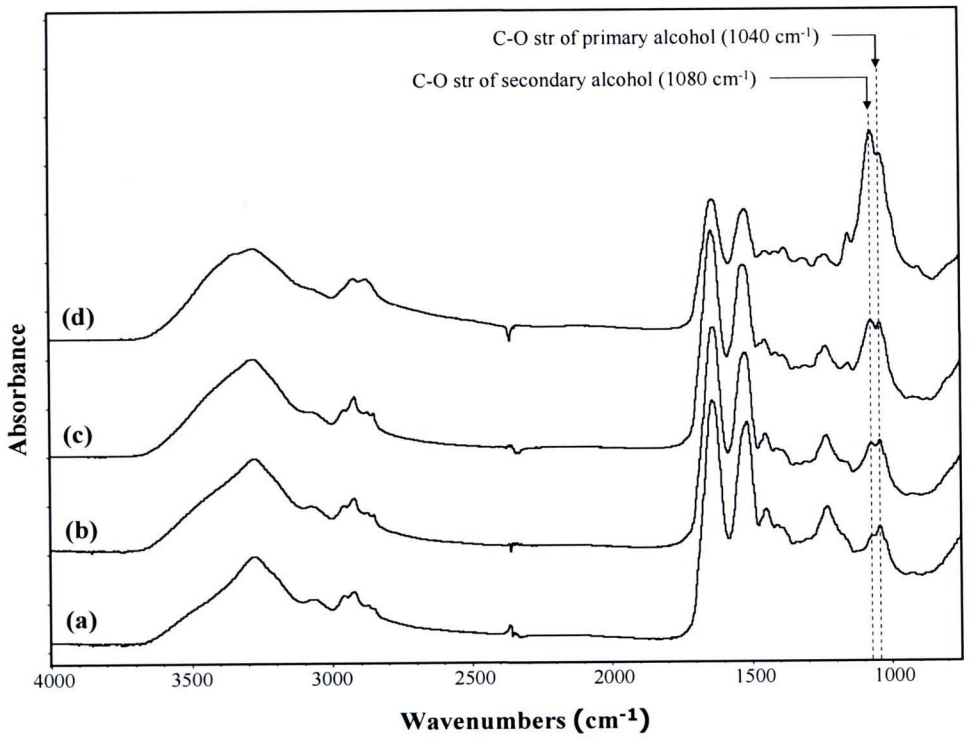

Figure 4-8 ATR FT-IR spectra of (a) virgin hair, (b) coated hair with 1%w/w HTACC (24%*DQ*) solution, (c) coated hair with 2%w/w HTACC (24%*DQ*) solution, and (d) coated hair with 3%w/w HTACC (24%*DQ*) solution.

Microscopic surface of virgin and treated-hair before and after the treatment with 1%w/w chitosan, TMC (22%*DQ*) or HTACC (24%*DQ*) solution were analyzed by SEM as shown in Figures 4-9 to 4-13. The negative charge on the surface hair is attracted to the $-NH_3^+$ group of chitosan and positively charged chitosan. Coating these treated-hairs, especially the waved and straightened hairs, by the polymer solution can flatten the lifted cuticle scales, occurred after the cosmetically treatments or UV irradiation. It is thus believed that the treated-hair can be physically "repaired" by the treatment with the chitosan and derivative solutions.

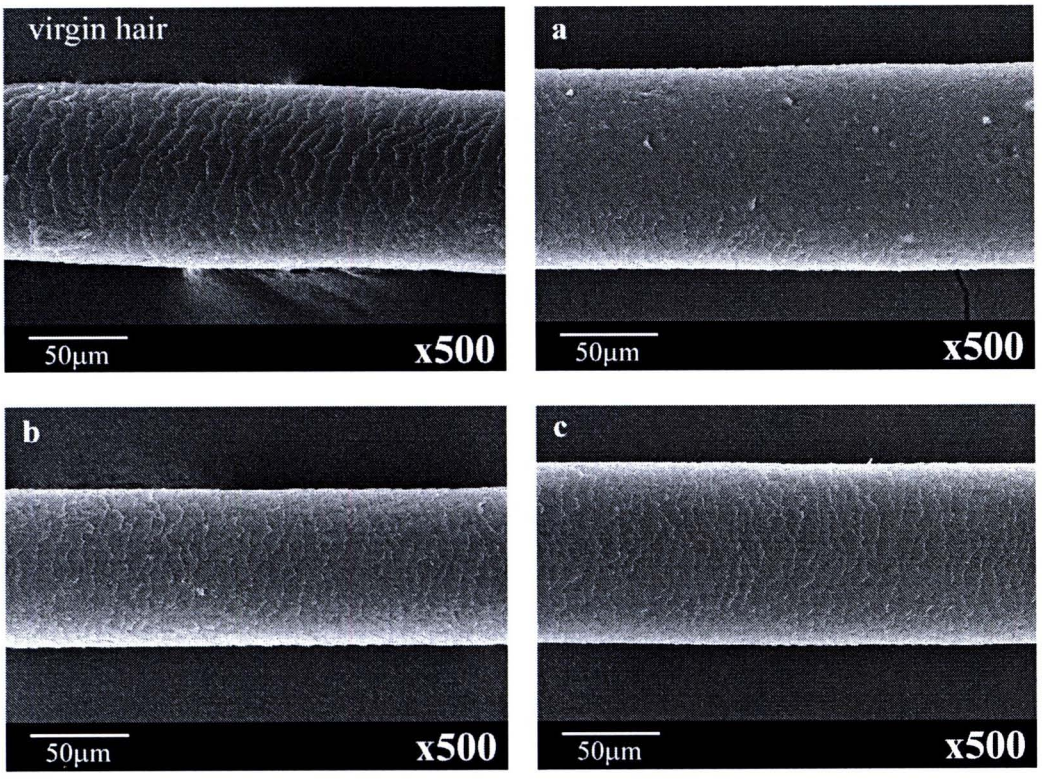

Figure 4-9 SEM images of virgin hair before and after treatment with (a) 1%w/w chitosan, (b) 1%w/w TMC (22%*DQ*) and (c) 1%w/w HTACC (24%*DQ*).

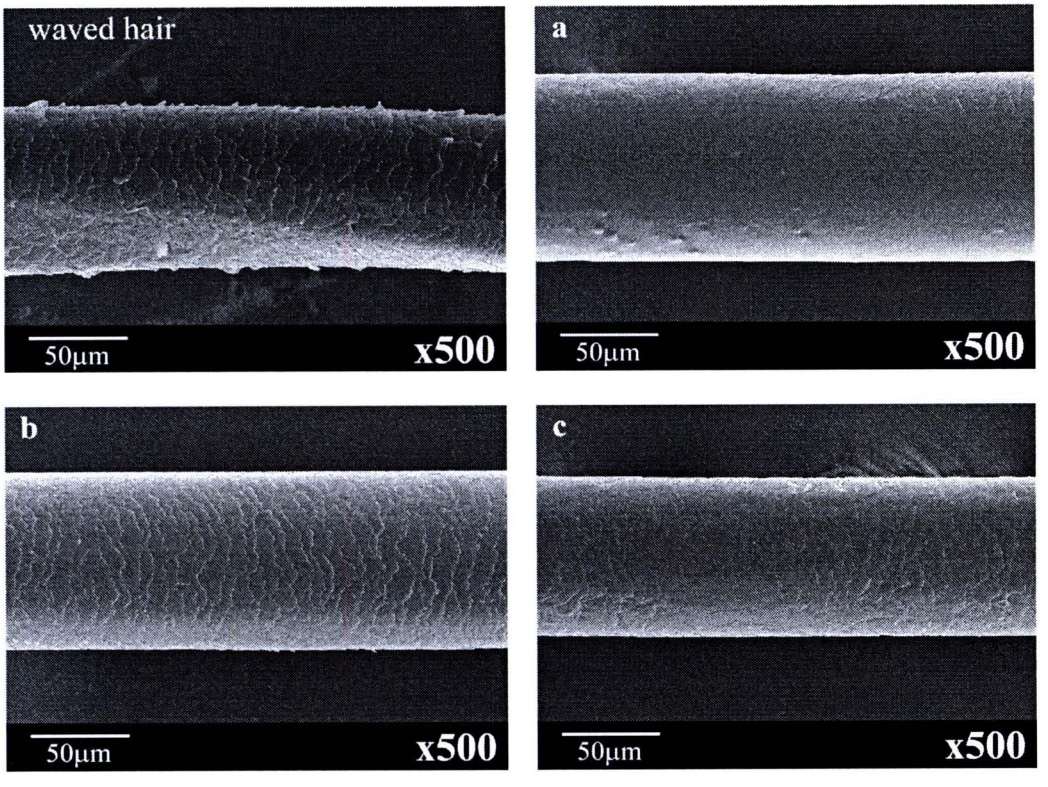

Figure 4-10 SEM images of waved hair before and after treatment with (a) 1%w/w chitosan, (b) 1%w/w TMC (22%*DQ*) and (c) 1%w/w HTACC (24%*DQ*).

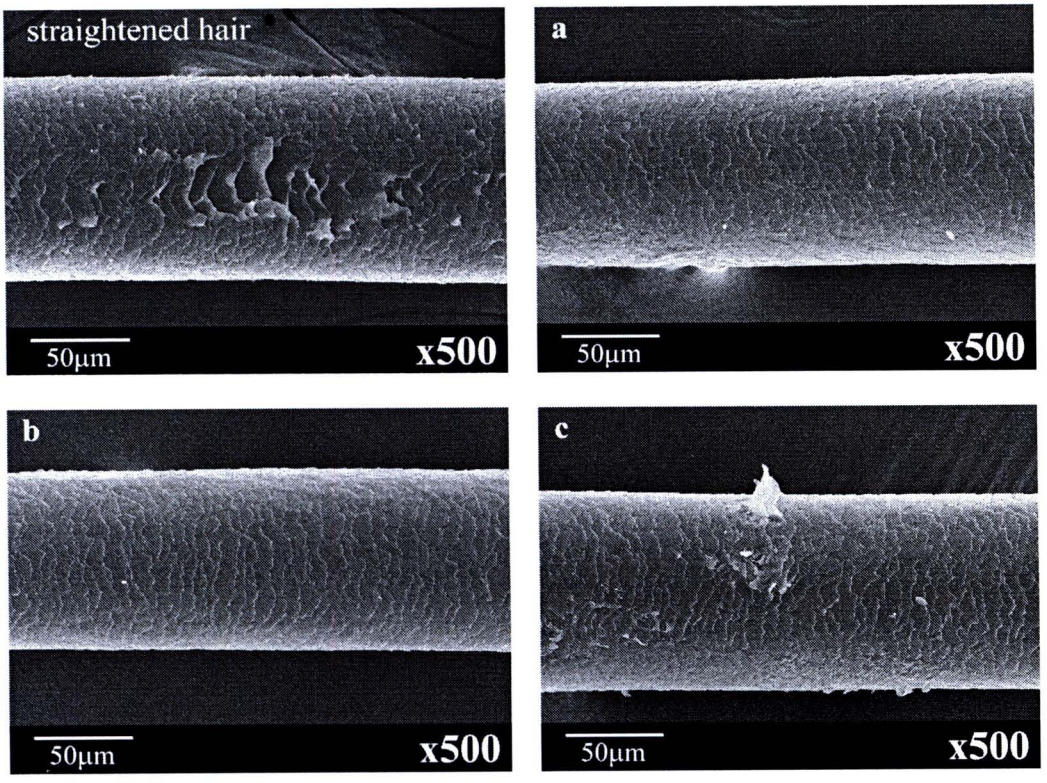

Figure 4-11 SEM images of straightened hair before and after treatment with (a) 1%w/w chitosan, (b) 1%w/w TMC (22%*DQ*) and (c) 1%w/w HTACC (24%*DQ*).

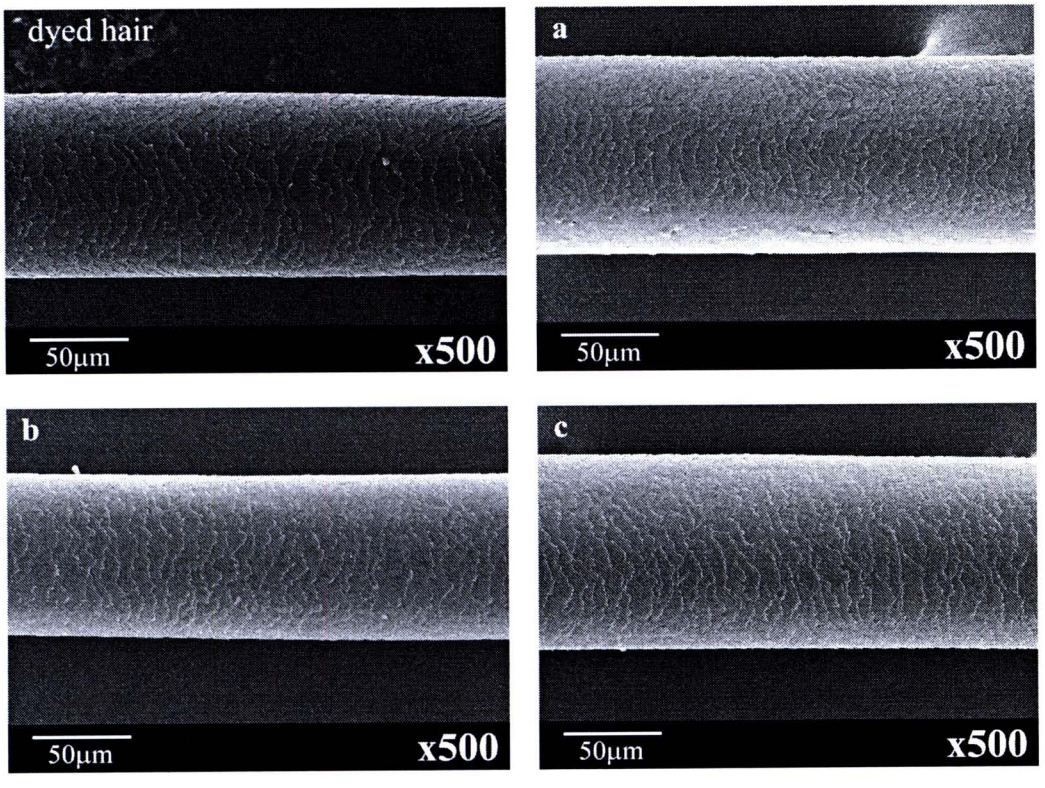

Figure 4-12 SEM images of dyed hair before and after treatment with (a) 1%w/w chitosan, (b) 1%w/w TMC (22%*DQ*) and (c) 1%w/w HTACC (24%*DQ*).

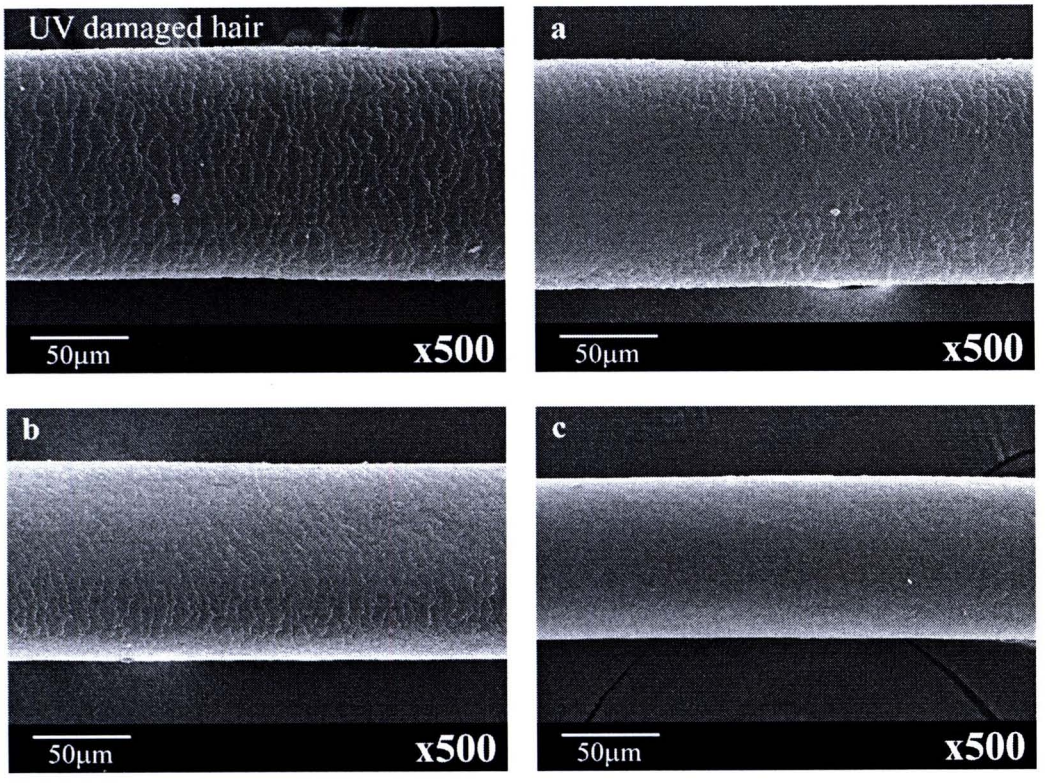

Figure 4-13 SEM images of UV-damaged hair before and after treatment with (a) 1%w/w chitosan, (b) 1%w/w TMC (22%*DQ*) and (c) 1%w/w HTACC (24%*DQ*).

From the results in section 4.2.1, 1-3%w/w chitosan and its derivatives can coat on the virgin and treated hairs surfaces as confirmed by ATR FT-IR and SEM analyses. Consequently, 1-3%w/w chitosan, TMC, and HTACC were used in preparing the leave-on conditioners.

4.2.2 Homogeneity and viscosity of leave-on conditioner

From the three concentrations 1-3%w/w, only the 1%w/w solution of chitosan, TMC or HTACC could be mixed into the conditioner to obtain good homogeneity. The conditioner creams tended to aggregate and form lumps when the concentration of polymer solution was 2 and 3%w/w. For comparison purpose, the conditioner without positively charged polymer (LO) and the one with 1%w/w polyquaternium-10 (LO+1%quat), as in a commercial product, were also investigated. Figure 4-14 shows the texture of five conditioner formulas. The natural color of chitosan is rather yellow therefore affecting the color of the prepared leave-on conditioners.

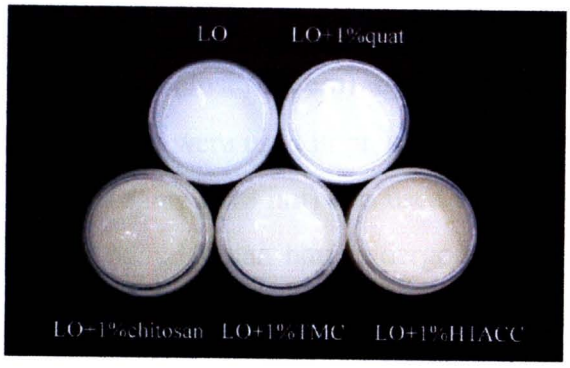

Figure 4-14 The appearance of the leave-on conditioner without positively charged polymer (LO), the leave-on with 1%w/w polyquaternium-10 (LO+1%quat), 1%w/w chitosan (LO+1%chitosan), 1%w/w TMC (LO+1%TMC), and 1%w/w HTACC (LO+1%HTACC).

The viscosity of the prepared five leave-on conditioners was analyzed by Brookfield Digital Viscometer model DV-I+. The condition of parameters as follows: spindle, speed, time, and temperature are S5, 60 rpm, 120 s, 25°C, respectively. The results are shown in Table 4-7. LO+1%TMC (3646 mPa.s) and LO+1%HTACC (3305 mPa.s) have low viscosity values because the solubilities of the two chitosan derivatives are higher than that of chitosan. Furthermore, the conditioners containing TMC or HTACC have lower viscosity values than does the conditioner containing polyquaternium-10. This characteristic should make the hair coated with LO+1%TMC and LO+1%HTACC feel more smooth than that coated with LO+1%quat as can be evidenced from the result of wet combing test shown in section 4.4.5.

Table 4-7 pH and viscosity of five leave-on conditioners.

Types of leave-on conditioner	pH	average ± SD (mPa.s)
LO	4.85	3611 ± 68
LO+1%quat	4.89	4526 ± 122
LO+1%Chitosan (85%*DD*)	4.51	4709 ± 81
LO+1%TMC (22%*DQ*)	4.81	3646 ± 40
LO+1%HTACC (24%*DQ*)	4.80	3305 ± 150

4.3 Functional Group and Microscopic Image Analysis of Hair Samples

Angela™ Cold wave lotion (Just Modern), Caring® Hair straightener cream, and Caring® Beauty hair colour cream were used in preparation of waved, straightened, and dyed hairs, respectively. A UV lamp (313 nm) was used as a UVB source for irradiation to prepare the UV-damaged hair. Human hair undergoes oxidation by both chemical treatment (permanent waves, straightener cream, or permanent dyes) and photochemical (exposure to UV radiation). Oxidation usually affects the decreased tensile strength of hair due to disulfide (–SS–) scission and the color changes, caused by melanin degradation and abraded cuticle.

The usual products from –SS– oxidation of cystine are the sulfonic acid of cystine or cysteic acid (R-SO_2-OH), cystine monoxide (R-SOS-R) and cystine dioxide (R-SO_2S-R), with IR absorption bands at 1040, 1075 and 1125 cm^{-1}, respectively (see structure in Figure 4-15).

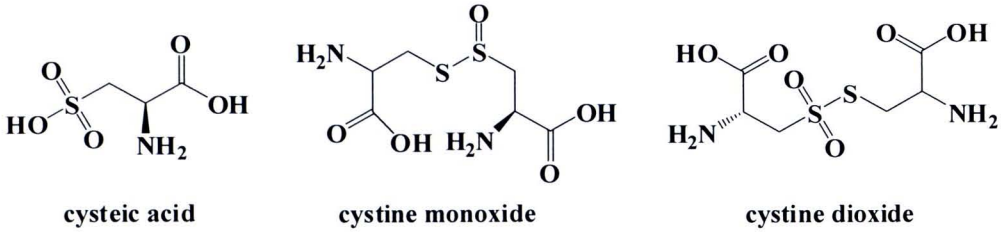

Figure 4-15 Structure of cysteic acid, cystine monoxide, and cystine dioxide.

An oxidizing agent in permanent wave, hair straightener cream, and hair coloring caused an increase in cysteic acid contents. In addition, weathering (exposure to sunlight or wind), could also increase the content of the cysteic acid as can be evidenced from the band intensity at 1040 cm^{-1}.[63]

However, reports by other researchers on the changing of virgin and damaged hairs are still different in comprehensiveness. In this work, cysteic acid contents and secondary structure of protein in hair samples were explored in detail using ATR FT-IR technique.

As a result, the spectra of different treated hairs in the 1070-1020 cm^{-1} region are somewhat different, indicating the difference in cysteic acid content of the keratin protein samples. This suggests that the partial –SS– groups on the surface of virgin hair has changed to cysteic acid through oxidation. The results from the ATR FT-IR analysis

(as shown in Figure 4-16) demonstrate that the oxidation has proceeded to a depth of at least 1-2 μm (estimated depth of ATR-FTIR sensitivity). The depth of 1-2 μm from surface corresponds to the cuticle region.

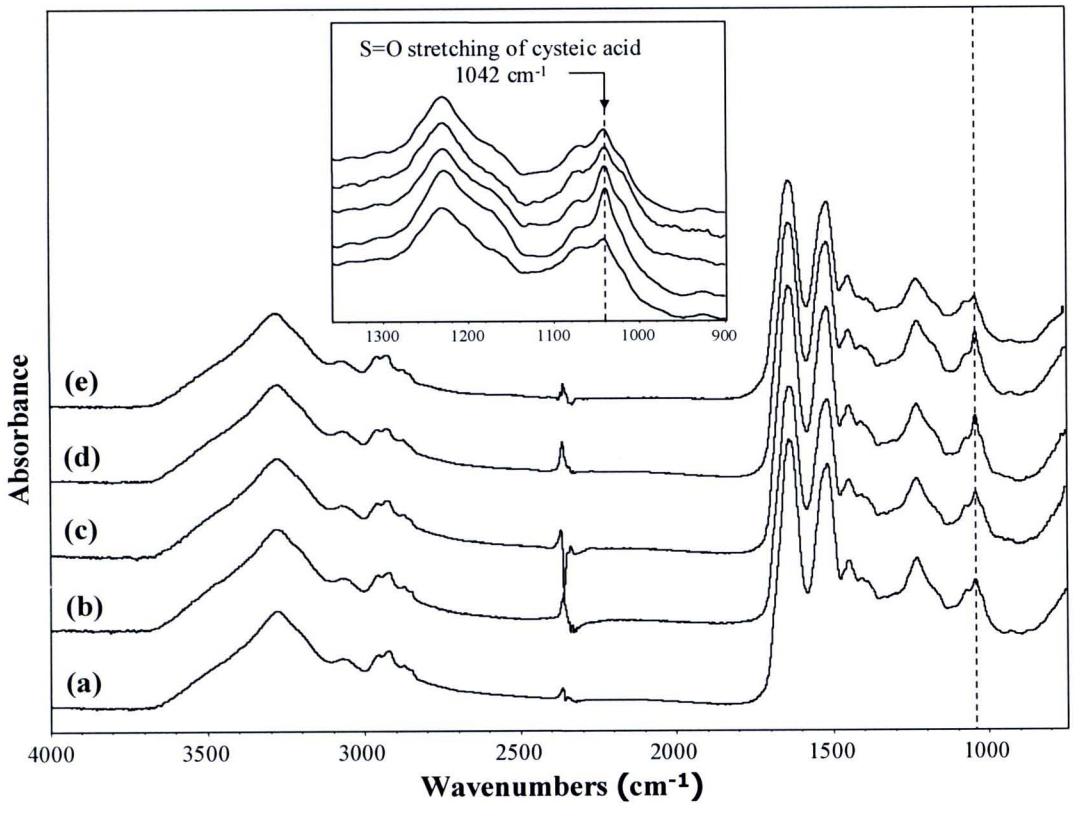

Figure 4-16 ATR-FTIR spectra of (a) virgin hair, (b) waved hair, (c) straightened hair, (d) dyed hair, and (e) UV-damaged hair.

The cysteic acid contents in all human hair types are compared. The normalization of ATR FT-IR spectra of keratin protein samples is carried out based on the amide I region at 1641 cm^{-1}, in which the peak area is large and not influenced by chemical treatment. The comparison of the peak area ratios of S=O stretching and amide I for virgin and treated-hairs is shown in Table 4-8. From the Table, the cysteic acid contents of treated-hairs are higher than that of the virgin hair. The cysteic acid contents of the dyed hair in cuticle region are increased remarkably. This result implicates that the –SS– groups in hair decrease which in fact can affect the tensile strength of hair (see section 4.4.3).

Table 4-8 Cysteic acid contents in virgin and treated-hairs.

Type of hair	n	Peak area		Cysteic acid contents[c]	Average ± SD
		amide I[a]	S=O[b]		
Virgin	1	14.170	0.340	0.0240	0.0227 ± 0.0011
	2	13.102	0.289	0.0221	
	3	13.475	0.296	0.0220	
Waved	1	4.962	0.125	0.0252	0.0244 ± 0.0015
	2	14.274	0.323	0.0226	
	3	13.892	0.351	0.0253	
Straightened	1	11.195	0.376	0.0336	0.0301 ± 0.0030
	2	11.536	0.331	0.0287	
	3	11.718	0.330	0.0282	
Dyed	1	7.183	0.286	0.0398	0.0438 ± 0.0038
	2	14.316	0.633	0.0442	
	3	14.397	0.682	0.0474	
UV damaged	1	6.086	0.144	0.0237	0.0276 ± 0.0049
	2	11.992	0.311	0.0259	
	3	14.412	0.478	0.0331	

[a]peak integration range is 1730-1580 cm^{-1}

[b]peak integration range is 1070-1020 cm^{-1}

[c]peak area ratios, S=O/amide I

Protein generally contains more than one secondary structures, which are correlated to the amide groups of protein. Secondary structures are associated with a characteristic pattern of hydrogen bonding between amide C=O and N–H groups. The secondary structures of protein can be classified as α-helix, β-sheet, β-turns, and random coil. The second derivative spectra were calculated to identify the positions of

the overlapping component bands in the amide I region (1730-1580 cm^{-1}) of which were used as initial parameters for curve fitting analysis.

The number and location of individual bands obtained from the second derivative of original (dotted line) spectrum were used in curve fitting as shown in Figure 4-17. The peak positions of secondary structure were calculated from deconvolved (solid line) spectrum. Absorption centers of curve fitting of virgin and treated-hairs, which can be referred from Table 4-9, were shown in Table 4-10. The secondary structure of virgin hair at 1650, 1615 and 1696, 1625, 1667 and 1684, and 1639 cm^{-1} are assigned to α-helix, antiparallel β-sheets, parallel β-sheets, β-turn, and random coil, respectively. These peaks are slightly shifted from those observed in treated-hairs, which might be due to the difference of hydrogen bonding of protein. The secondary structure of treated-hairs are represented by positive shift of individual bands in amide I bands as shown in Table 4-11. Although the curve fitting is the same for all type, the proportions of secondary structure depend on the type of treatment. When the virgin hair is treated chemically or by UVB irradiation, the structure was changed from α-helix to β-sheet or random coil. α-Helix structure (18.3%) is more favorable in virgin hair. Similarly, antiparallel β-sheets (27.5%) is highly populated in waved hair, and parallel β-sheets (28.1%) is highly populated in UV damaged hair. Straightened hair has more random coil structure (28.2%) than other type of hair. It should be noted that changing of secondary structure could be only analyzed in the cuticle region.

Table 4-9 Amide I band frequencies and assignments to secondary structure for protein.[64,65]

Assignments	Wavenumbers (cm^{-1})	
	Literature 1[64]	Literature 2[65]
α-helix	1650-1657	1651
Antiparallel β-sheets	1612-1640, 1670-1690 (weak)	1611-1631
Parallel β-sheets	1626-1640	1622-1645
β-turn	1655-1675, 1680-1696	1668-1680, 1690-1692
Random coil	1640-1651	1668-1680

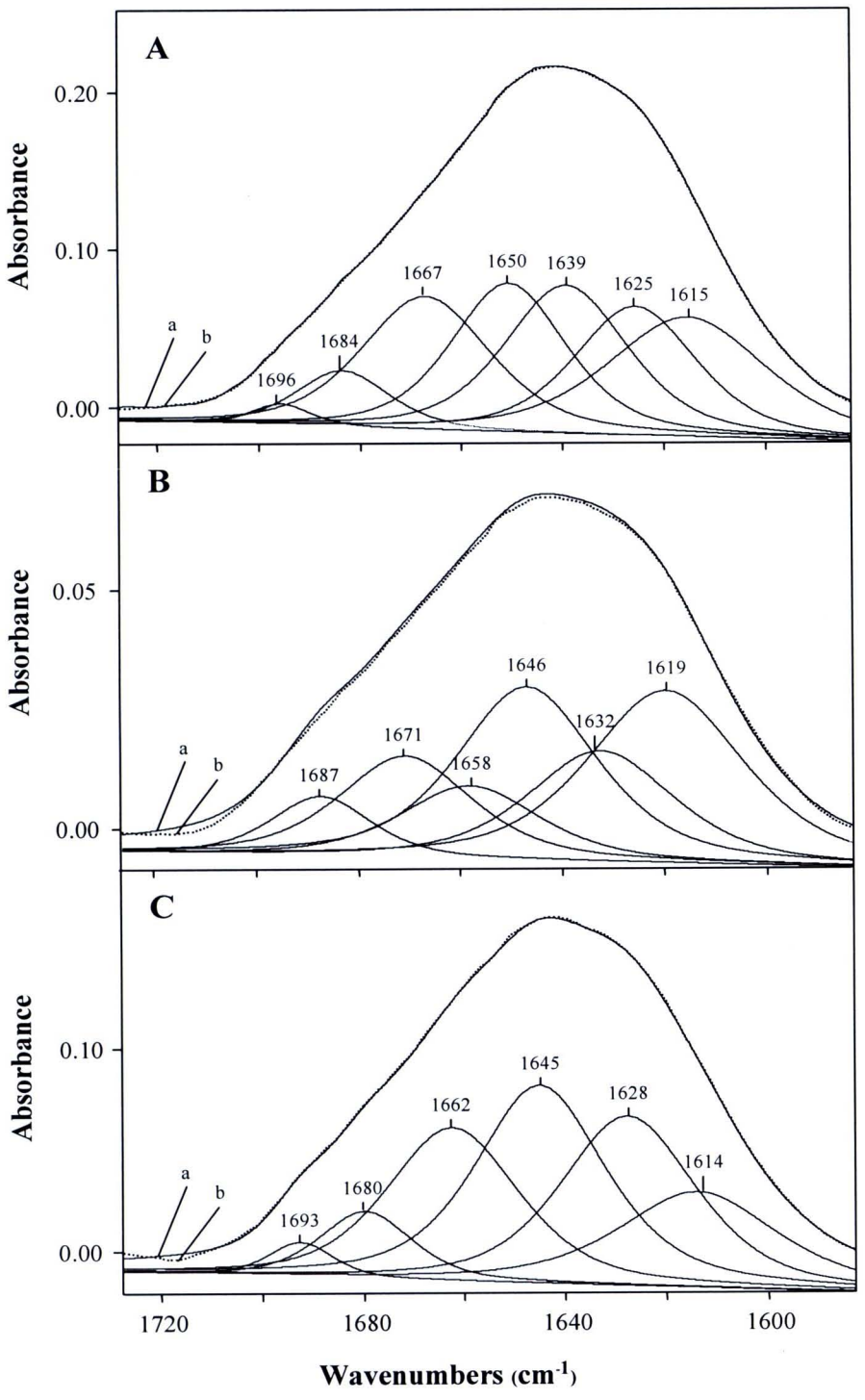

Figure 4-17 Curve fitting of the amide I region of the cuticle spectrum (depth of 1-2 μm from the hair surface) of (A) virgin hair, (B) waved hair, (C) straightened hair, (D) dyed hair, and (E) UV-damaged hair: (a) deconvolved (solid line) spectrum and (b) original (dotted line) spectrum.

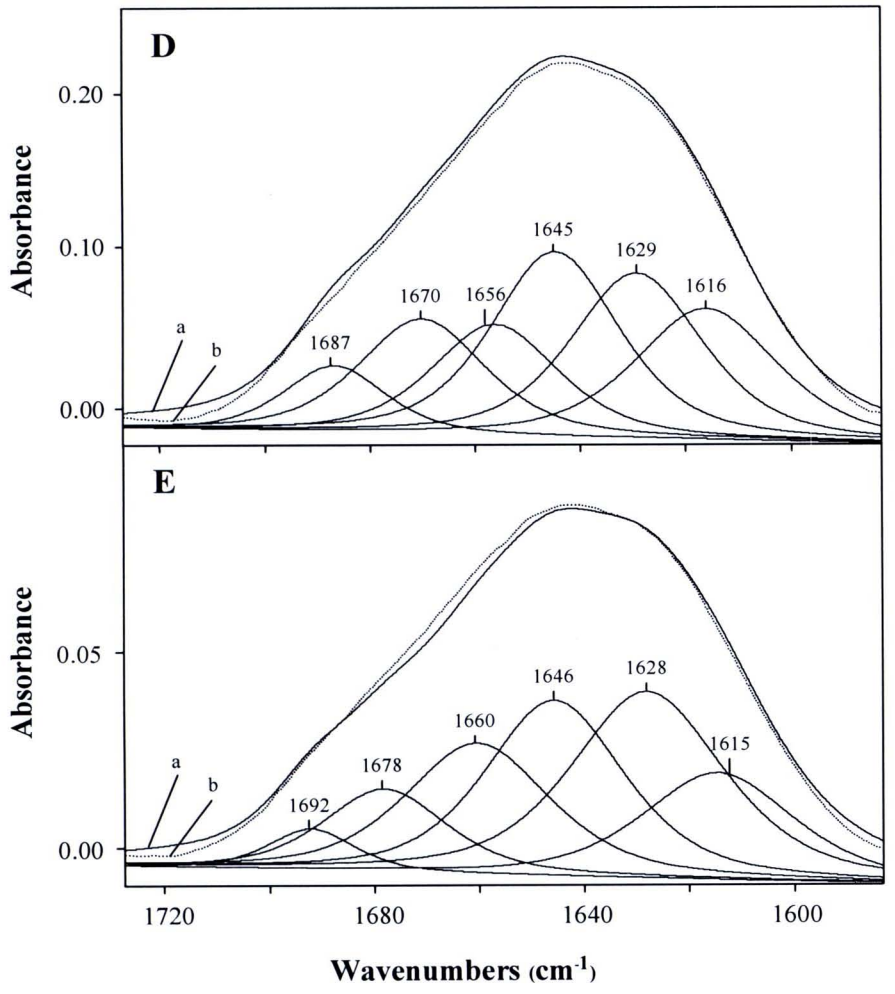

Figure 4-18 *continued*

Table 4-10 The number and location of individual bands obtained from second derivative of virgin and treated-hair.

Types of hair	Assignments (current work)									
	α-helix		Antiparallel β-sheets		Parallel β-sheets		β-turn		Random coil	
	Wavenumber (cm^{-1})	Area (%)	Wavenumber (cm^{-1})	Area (%)	Wavenumber (cm^{-1})	Area (%)	Wavenumber (cm^{-1})	Area (%)	Wavenumber (cm^{-1})	Area (%)
Virgin hair	1650	18.3	1615, 1696	21.6	1625	16.7	1667, 1684	23.9	1639	19.4
Waved hair	1658	10.6	1619	27.5	1632	16.6	1671, 1687	20.2	1646	25.1
Straightened hair	1662	21.4	1614, 1693	19.4	1628	24.3	1680	6.6	1645	28.2
Dyed hair	1656	14.3	1616	18.6	1629	21.7	1670, 1687	21.7	1645	23.7
UV-damaged hair	1660	18.7	1615, 1692	19.3	1628	28.1	1678	10.1	1646	23.8

Furthermore, the morphological surface of virgin and treated-hairs was investigated by SEM as shown in Figure 4-18. The morphological surface of waved and straightened hairs in cuticle region was changed remarkably. The morphology of cuticle region of the dyed hair was not changed significantly, possibly due to the fact that the hair surface was coated by the pigment color. The UV-damaged hair also seemed to be unaffected. These results suggest that only some treatment methods can cause physical damage on the hair surface. Nonetheless, all treatment affected the chemical structure at molecular level of hair, as previously confirmed by ATR FT-IR technique.

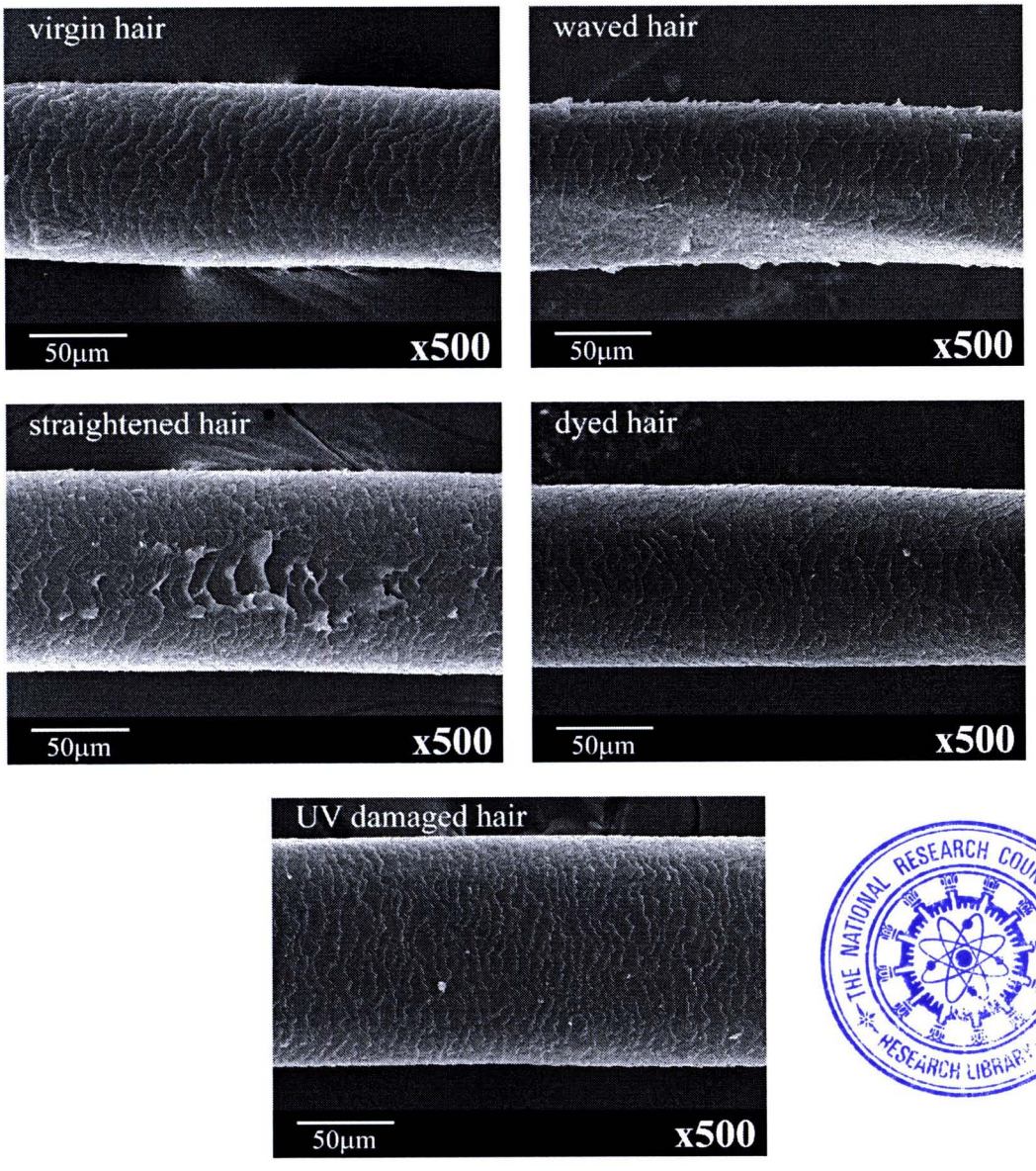

Figure 4-18 SEM images of virgin, waved, straightened, dyed, and UV-damaged hairs.

4.4 Physical and Mechanical Properties of Conditioner-Coated Hairs.

This part was divided into five parts. The two parts cover the ATR FT-IR and SEM analysis of coated hairs with five conditioner formula. The remained three parts are dedicated to the evaluation of the conditioner-coated hairs in term of tensile properties, hair texture, and resistant to wet combing.

4.4.1 ATR-FTIR spectra of conditioner-coated hairs

The ATR-FTIR spectra of the conditioner-coated hairs are shown in Figure 4-19. By comparison, the observed spectra of all coated hairs with various leave-on conditioners show different spectral feature at 2851-2957 cm^{-1} and 1000-1100 cm^{-1} from the virgin hair did. The peak intensity at 2851-2957 cm^{-1} increased because of the increasing $-CH_2-$ groups from the long chain alcohols and ester in the leave-on conditioners. Moreover, the intensities of C–O stretching signals of the alcohol at 1040 and 1080 cm^{-1} of almost all ingredients, such as glycerine, cetyl alcohol, stearyl alcohol, euxyl K300 (i.e. phenoxyethanol, methylparaben, ethylparaben, propylparaben, butylparaben, and *iso*-butylparaben) [see Figure 4-19(b)-(f)], are obviously higher than found in the untreated virgin hair. Besides, the peak intensity at 1000-1100 cm^{-1} also increases due to the –Si–O– in cyclomethicone in the conditioners [Figure 4-19(b)-(f)]. Furthermore, the peak intensity of O–H stretching at 3283 cm^{-1} increases due to glycerine and positively charged polymer, the highest content in the leave-on conditioners (see Figure 4-19).

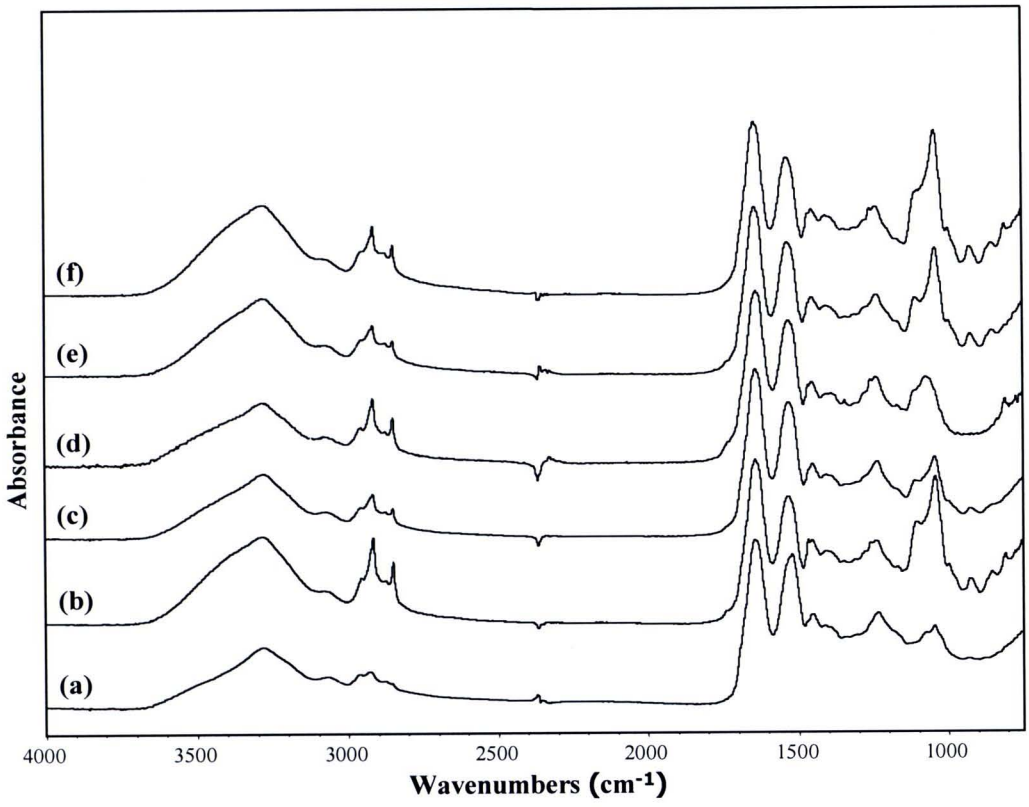

Figure 4-19 ATR-FTIR spectra of (a) virgin hair and the virgin hairs that were coated (b) LO, (c) LO+1%quat, (d) LO+1%chitosan, (e) LO+1%TMC, and (f) LO+1%HTACC.

4.4.2 Surface morphology of conditioner-coated hairs

The SEM images of virgin hairs that were coated by different leave-on conditioners were taken at 3-4 different positions along the hair strand. From Figures 4-20 to 4-24, patches of the conditioners are seen covering some or the whole areas of the hair strands. It is anticipated that the positively charged components in the conditioner should be attracted to the negative charged hair surface and therefore should somewhat affect the coating effectiveness of the conditioner. Apparently from SEM images in Figure 4-20, the leave-on conditioner without positively charged polymer (LO) cannot completely cover the hair fibers. On the other hand, the leave-on conditioners with cationic polymers (LO+1%quat, LO+1%chitosan, LO+1%TMC, or LO+1%HTACC) fully cover the hair surface (Figures 4-21 to 4-24). However, in case of the LO+1%chitosan-coated hair (Figure 4-22), the surface seems to be rougher than the others. This is probably because of the limited solubility of chitosan in the leave-on conditioner at the pH of conditioner (4.5-5.5) which is very close to the pKa (~6.5) of chitosan.

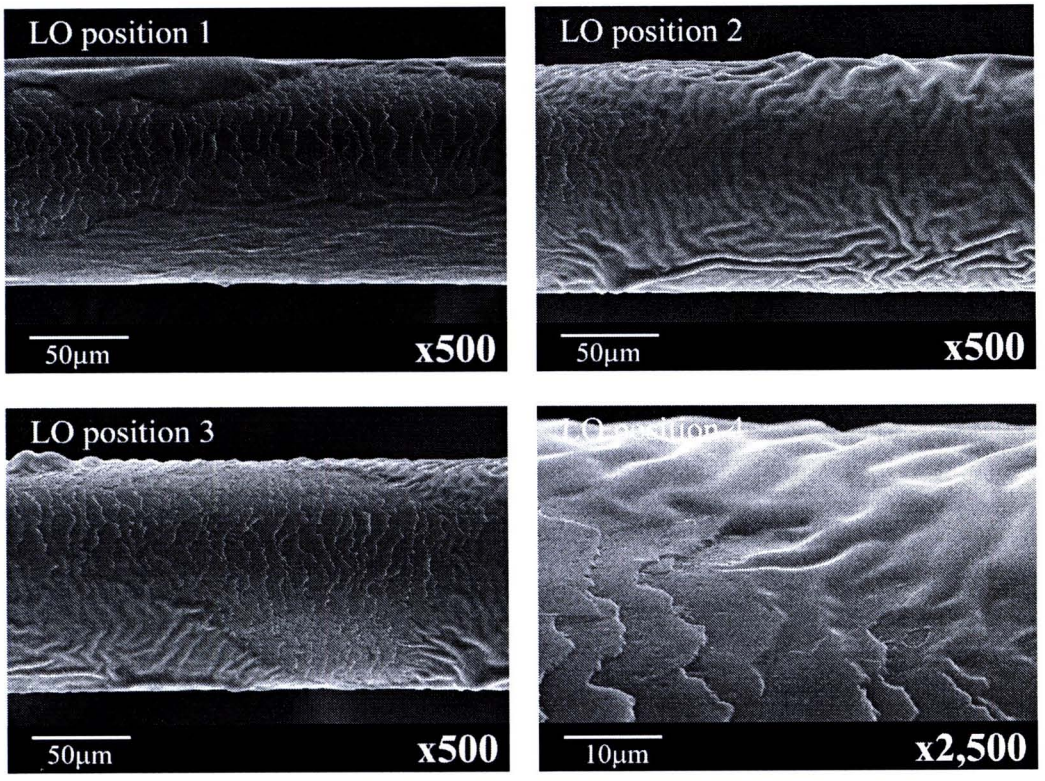

Figure 4-20 SEM images of virgin hair after the treatment with the leave-on conditioner without positively charged polymer.

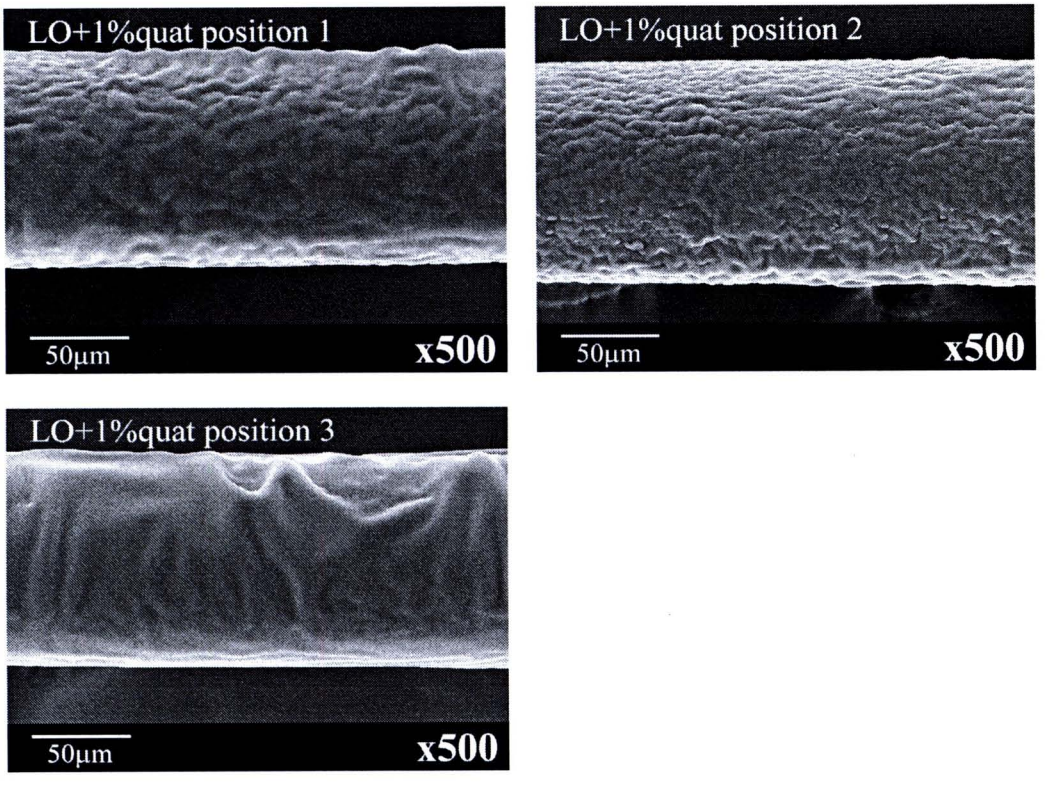

Figure 4-21 SEM images of virgin hair after the treatment with the leave-on conditioner containing 1%w/w polyquaternium-10.

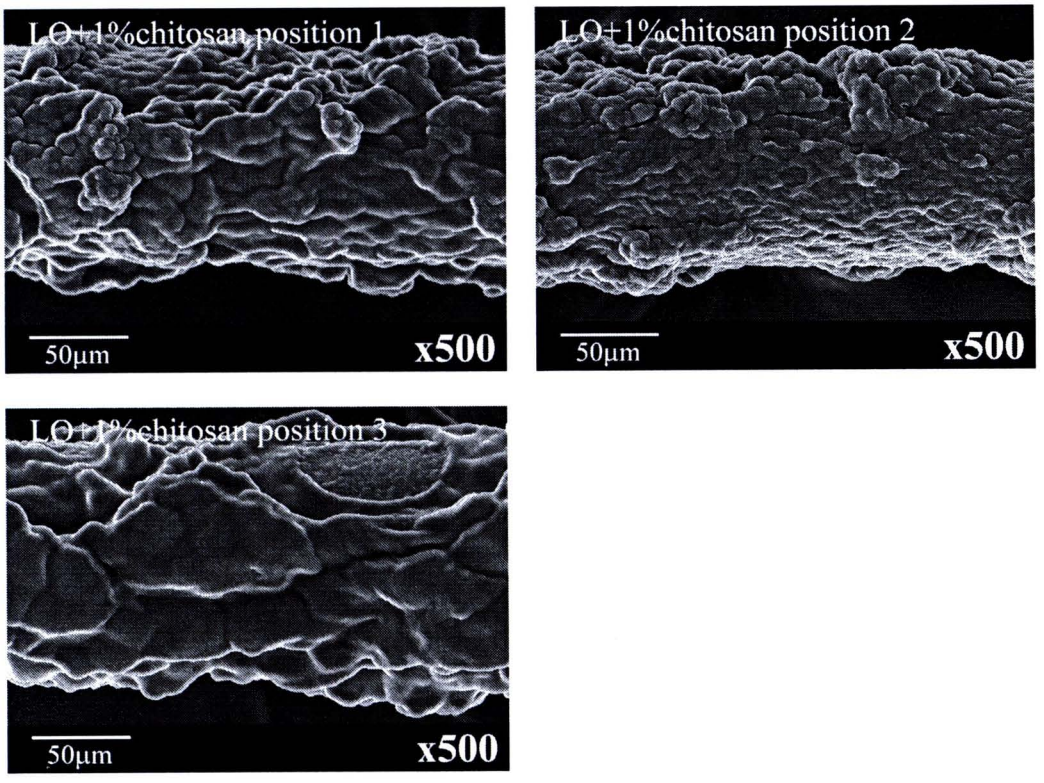

Figure 4-22 SEM images of virgin hair after the treatment with the leave-on conditioner containing 1%w/w chitosan.

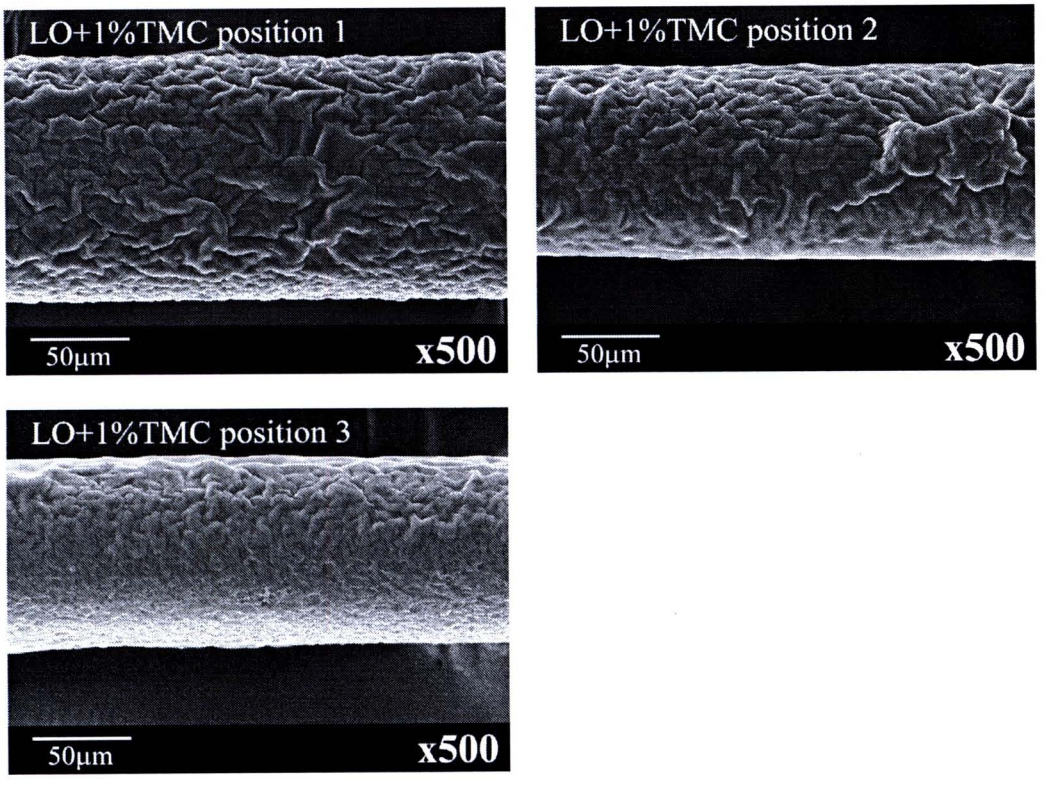

Figure 4-23 SEM images of virgin hair after the treatment with the leave-on conditioner containing 1%w/w TMC.

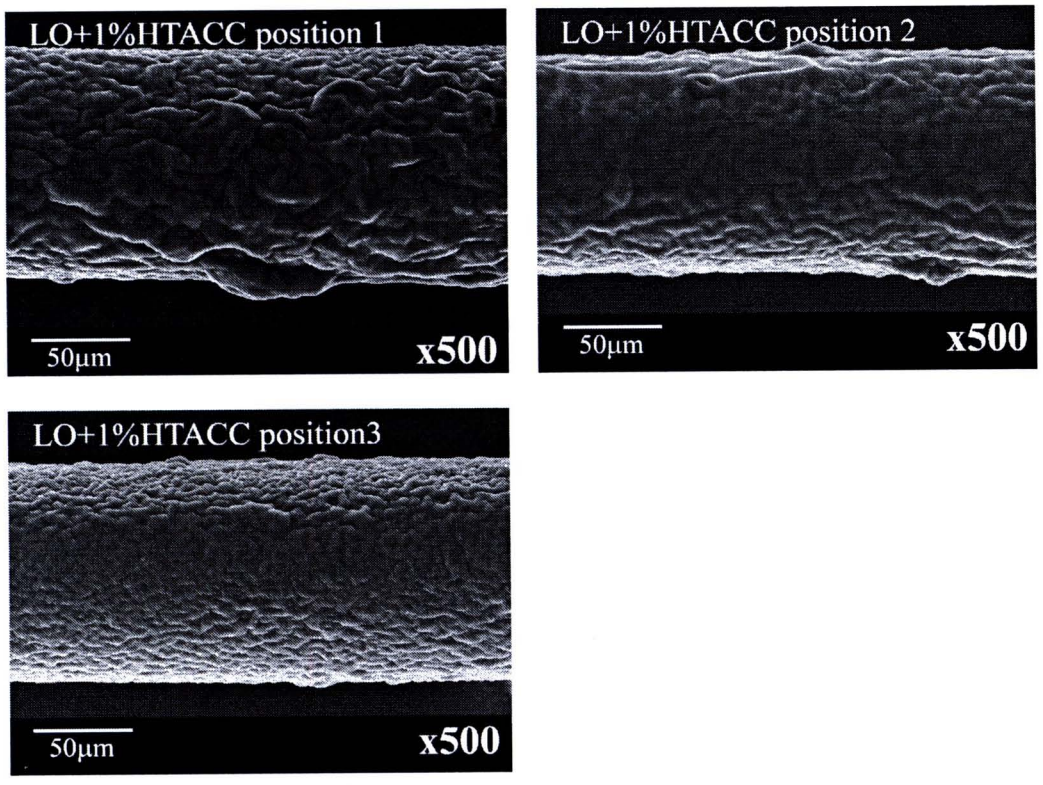

Figure 4-24 SEM images of virgin hair after the treatment with the leave-on conditioner containing 1%w/w HTACC.

4.4.3 Tensile properties of hair samples

This technique is used for measuring the tensile properties of keratin fiber that is related to the hair strength. The usual procedure for evaluating the tensile properties of keratin fiber is via load-elongation (stress/strain) method. The tensile test was performed at a fixed rate (20 mm/min), a fixed relative humidity (approximately 50%RH), and temperature (22°C). Figure 4-25 presents stress-strain curves for five hair types. The stress-strain curve of human hair is similar to that of wool and other keratinous fibers. When a keratin fiber is extended, the load elongation curve shows three distinct regions as marked in Figure 4-25. In the pre-yield region, also referred to as the Hookean region, the stress (load) is approximately linear to the strain (elongation). The ratio of stress to strain in this region is an elastic modulus. In this region, the resistance is provided by hydrogen bonds that are present between turns and stabilize the α-helix of keratin fiber. The yield region represents transition of keratin from α-form to β-form.[66] The chains unfold without any resistance, and hence the stress does not vary with strain. Typically, yield begins around 5% and post-yield begins at

around 25% strain. Then, the β-configuration again resists extension. Therefore, in the post-yield region, the stress again increases with strain until the keratin fiber breaks.

Table 4-11 presents the results from the tensile test of uncoated and coated hair by five leave-on conditioner formula. The parameters such as elastic modulus (N/m^2; Pa), plateau load (gmf/sq.μm), break extension (%strain), and break load (gmf/sq.μm) are reported. From the tensile tests of the uncoated virgin and damaged hairs, the elastic modulus and plateau loads are not significantly different from one another. The break load of the uncoated waved and straightened hairs are significantly different when compared with the virgin hair as shown in Figure 4-26. However, it is most likely that the chemical/UV treatment only affected the cuticle scales (as discussed in section 4.3), not the inner cortex part. In fact, the cortex contributes significantly to the tensile properties of hair.

Detailed comparison of virgin, waved, and straightened hairs reveals that the break load of the virgin hair is not affected by the presence of conditioner types. On the other hand, the break loads of the waved and straightened hairs increase significantly when the conditioners are applied (Figure 4-27). It is possible that the more uniform deposition and better covering of the leave-on conditioner layer on the hair strand than the virgin hair results in the increase of hair strength.

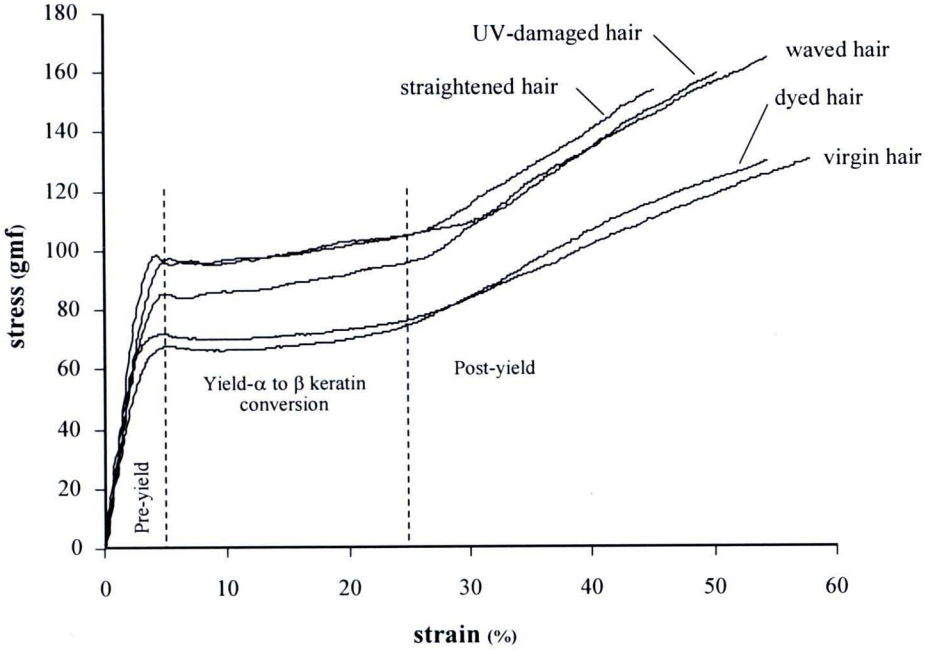

Figure 4-25 Stress-strain curves for five types of hair (virgin, waved, straightened hair, dyed hair, and UV-damaged hair).

Table 4-11 Tensile properties of uncoated and coated hair by five leave-on conditioner formula.

Hair types	Cross-sectional area (sq.μm)	Elastic modulus ($\times 10^9$ N/m^2; Pa)	Plateau load ($\times 10^{-2}$ gmf/sq.μm)	Break extension (%)	Break load ($\times 10^{-2}$ gmf/sq.μm)
Virgin hair	7124.7 ± 1221.4	2.76 ± 0.28	1.32 ± 0.03	57.19 ± 4.66	2.16 ± 0.06
LO-coated virgin hair	6094.4 ± 1356.3	2.61 ± 0.21	1.18 ± 1.25	49.91 ± 2.23	2.08 ± 0.08
LO+1%quat-coated virgin hair	4917.8 ± 1395.3	2.77 ± 0.22	1.20 ± 0.07	49.33 ± 3.81	2.14 ± 0.17
LO+1%chitosan-coated virgin hair	5749.5 ± 808.3	2.89 ± 0.33	1.23 ± 0.05	50.95 ± 4.02	2.12 ± 0.96
LO+1%TMC-coated virgin hair	6107.5 ± 1390.4	3.13 ± 0.97	1.22 ± 0.05	51.16 ± 5.96	2.17 ± 0.16
LO+1%HTACC-coated virgin hair	5954.5 ± 1367.9	3.03 ± 0.40	1.23 ± 0.04	51.05 ± 2.27	2.24 ± 0.13
Waved hair	6870.8 ± 1197.6	2.87 ± 0.33	1.21 ± 0.10	51.45 ± 7.4	1.88 ± 0.25
LO-coated waved hair	5697.9 ± 1078.9	2.96 ± 0.25	1.23 ± 0.05	49.91 ± 3.85	2.20 ± 0.12
LO+1%quat-coated waved hair	6168.6 ± 1085.3	2.85 ± 0.26	1.21 ± 0.06	49.18 ± 3.11	2.15 ± 0.17
LO+1%chitosan-coated waved hair	5760.8 ± 939.7	3.01 ± 0.29	1.25 ± 0.03	49.50 ± 4.80	2.21 ± 0.20

The values presented here are based on 10 measurements.

Table 4-11 *continued*

Hair types	Cross-sectional area (sq.μm)	Elastic modulus ($\times 10^9$ N/m^2; Pa)	Plateau load ($\times 10^{-2}$ gmf/sq.μm)	Break extension (%)	Break load ($\times 10^{-2}$ gmf/sq.μm)
LO+1%TMC-coated waved hair	6241.6 ± 1680.1	3.05 ± 0.35	1.23 ± 0.06	49.69 ± 3.98	2.22 ± 0.17
LO+1%HTACC-coated waved hair	5767.6 ± 1584.4	3.12 ± 0.26	1.25 ± 0.04	49.10 ± 2.90	2.26 ± 0.12
Straightened hair	7506.9 ± 1391.5	3.08 ± 0.39	1.18 ± 0.08	51.62 ± 8.0	1.83 ± 0.23
LO-coated straightened hair	6423.1 ± 878.9	3.00 ± 0.71	1.29 ± 0.23	46.97 ± 4.38	2.20 ± 0.28
LO+1%quat-coated straightened hair	7440.5 ± 1180.6	2.93 ± 0.27	1.19 ± 0.05	49.83 ± 6.17	2.11 ± 0.17
LO+1%chitosan-coated straightened hair	7167.4 ± 1486.6	2.95 ± 0.28	1.20 ± 0.06	49.16 ± 4.32	2.14 ± 0.17
LO+1%TMC-coated straightened hair	7221.9 ± 1220.0	3.05 ± 0.33	1.22 ± 0.07	48.82 ± 2.23	2.18 ± 0.17
LO+1%HTACC-coated straightened hair	4677.0 ± 706.8	3.09 ± 0.32	1.26 ± 0.03	45.68 ± 2.76	2.25 ± 0.07
Dyed hair	7438.4 ± 1025.8	3.12 ± 0.41	1.35 ± 0.04	49.92 ± 6.0	2.08 ± 0.17
UV-damaged hair	7303.1 ± 1506.3	3.07 ± 0.43	1.28 ± 0.05	50.23 ± 6.7	2.06 ± 0.25

The values presented here are based on 10 measurements.

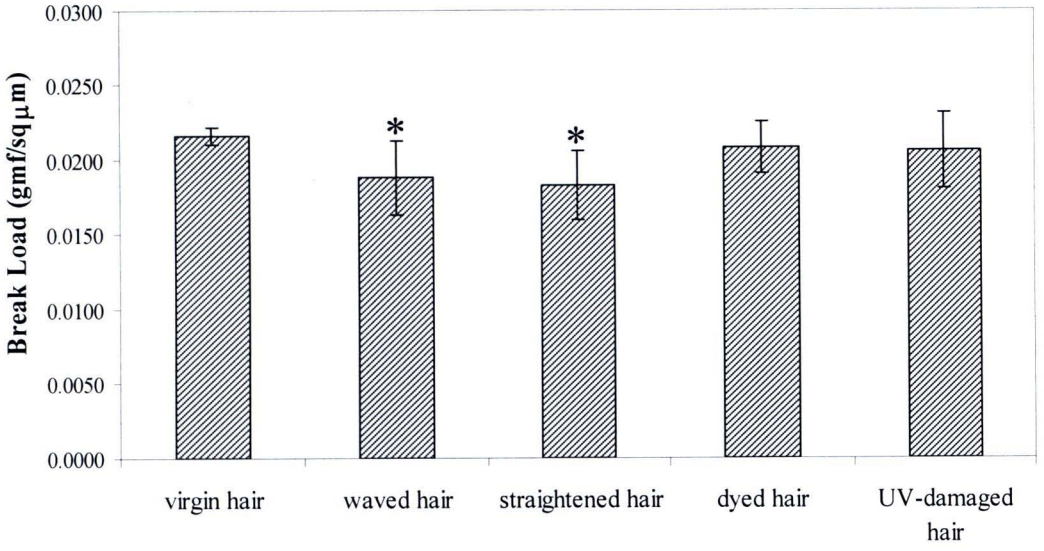

Figure 4-26 Break load of virgin, waved, straightened, dyed and UV-damaged hairs. $^{*}p < 0.05$ (compared to virgin hair).

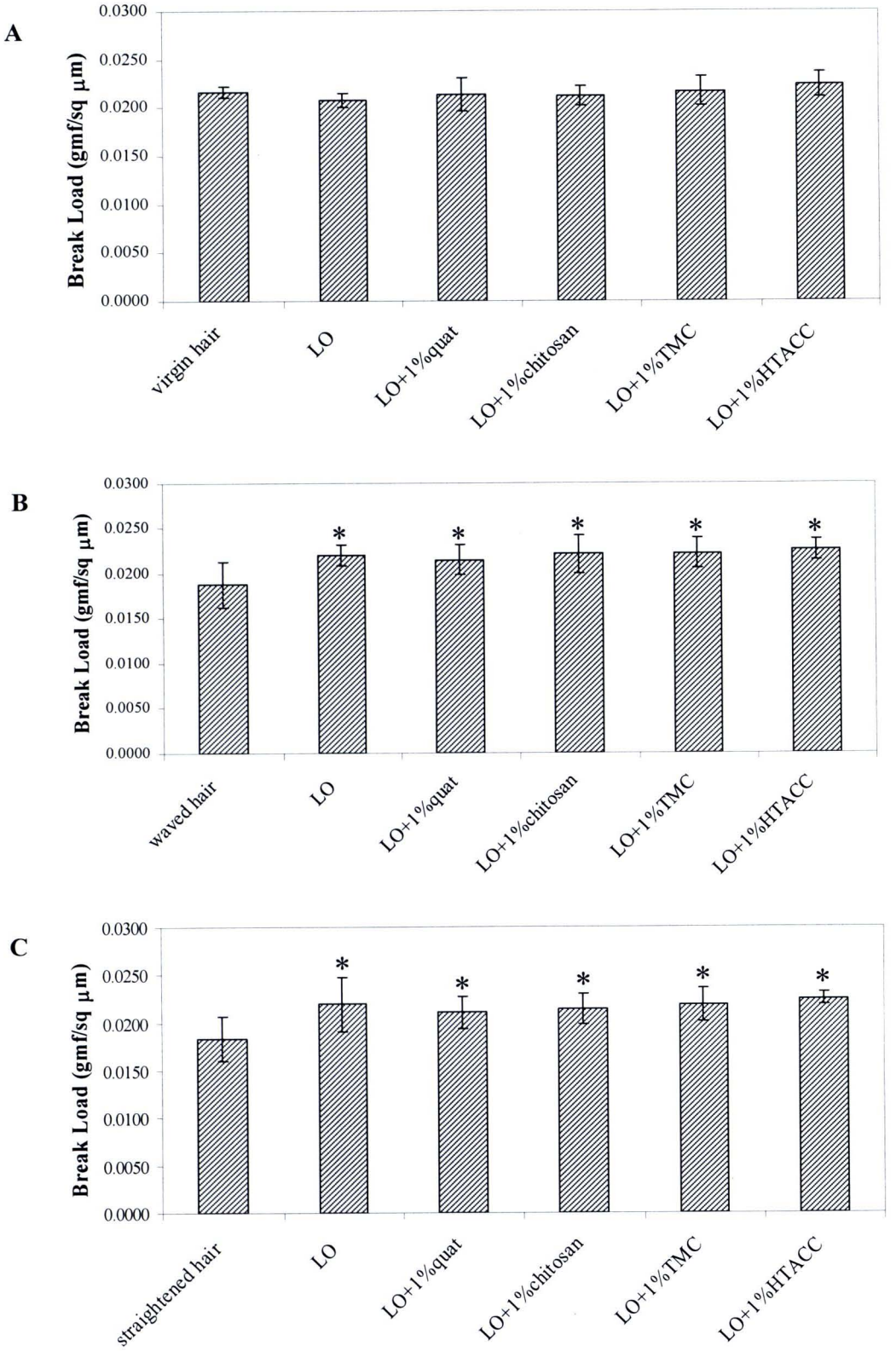

Figure 4-27 Comparison of break load of (A) virgin, (B) waved, and (C) straightened hairs with and without treatment by five leave-on conditioners. $^{*}p < 0.05$ (compared to non-treated hair). The values presented here were averaged from 10 measurements.

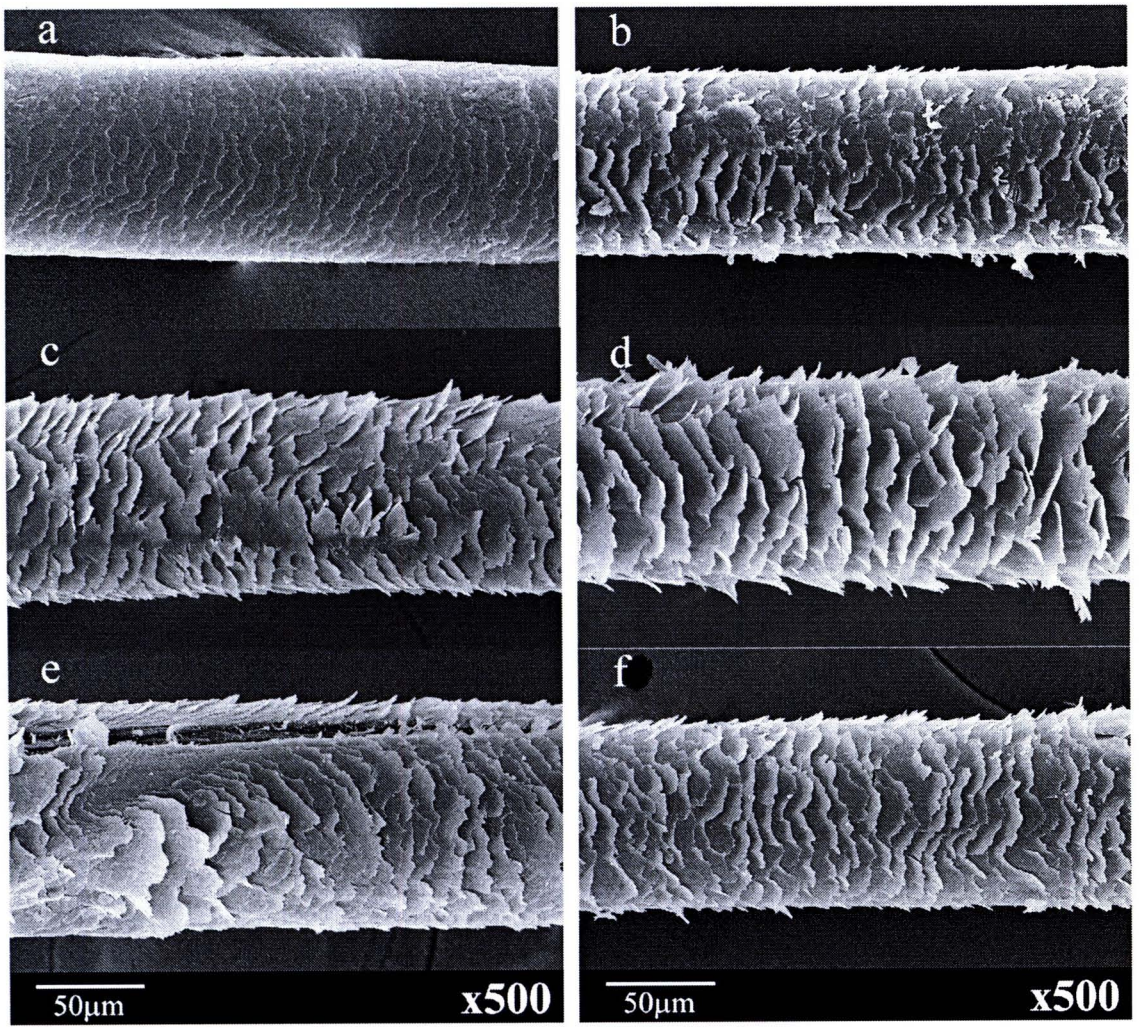

Figure 4-28 SEM images of fractured cuticle scales of virgin hair caused by hair extension at 50% relative humidity: (a) original virgin hair, tensile tested samples: (b) virgin, (c) waved, (d) straightened (e) dyed, and (f) UV-damaged hairs.

Figure 4-28 displays the SEM images of fractured in the cuticle scales. The cuticle scales of all broken hairs are lifted. Upon closely inspection, the cuticle scales of all chemically treated hairs are lifted quite extensively as shown in Figure 4-28(c)-(e). It is however noted here that lifting of cuticle scales cannot be correlated directly with the obtained tensile test results.

Additionally, fibrillation, smooth, splitting, and step is usually the four most common fracture patterns for human hair. The fracture pattern generally depends on the extent of hair damage, the relative humidity, and whether the fiber is twisted or contains flaws. If the hair and its cuticle are in good condition (e.g., near the root end), a smooth break tends to occur.[1] As a result, the fracture pattern of the five hair types are random pattern (i.e. smooth, splitting, and step) as shown in Appendix C.

4.4.4 Hair texture analysis

This technique was used for measuring the friction force (g.mm) of hair surface that is directly related to the smooth or slippery feel on hair. In the procedure, a probe was passed through hair tresses surface at speed of 10 mm/sec and the friction force was measured as a function of distance. The friction forces are shown in Figure 4-29.

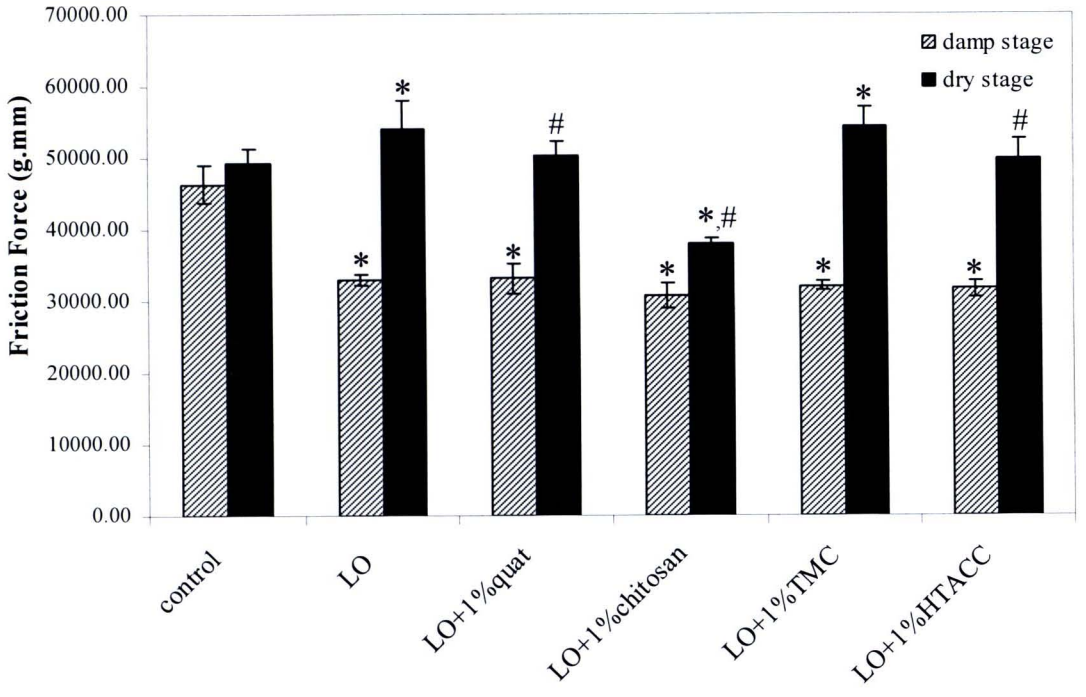

Figure 4-29 Comparison of the friction force of hair surface, subjected to treatment by five leave-on conditioner formula and DI water (control). $^{*}p < 0.05$ (compared to control) and $^{\#}p < 0.05$ (compared to LO). The values presented were averaged from 5 measurements.

The leave-on conditioner usually provides easier combing and detangling in both damp and dry conditions. Consequently, this study was carried out with hairs in both damp and dry stages. The results in Figure 4-29 are reported in terms of the friction force that is directly correlated to the smooth feel. The friction force in damp stage is always lower than in the dry stage. In the damp stage, the friction force is not significantly different when compared between each conditioners formula. However, in the dry stage, the friction force of hair coated with LO+1%chitosan is the lowest.

4.4.5 Wet combing test

This technique is used for measuring the friction force (gmf) generated upon combing conditioner-coated hair tresses with a metal comb to determine ease of combing and hair detangling. In the usual procedure, hair tresses are passed through a comb at a speed of 40 inch/min and the friction force is measured as a function of distance.

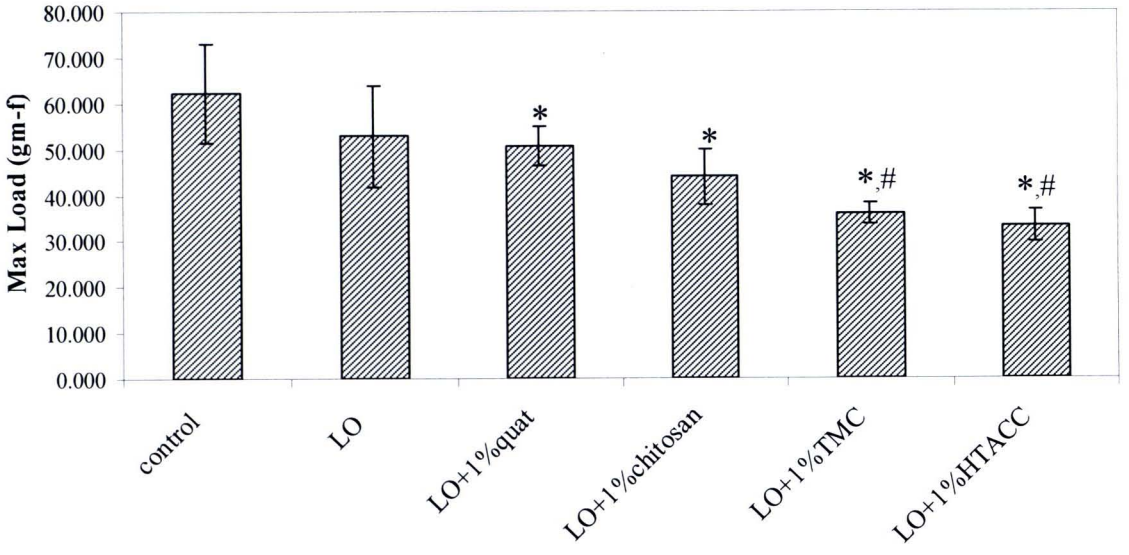

Figure 4-30 Comparison of max loads of hairs tresses subjected to treatment by five leave-on conditioner formulas and DI water (control). $^{*}p < 0.05$ (compared to control) and $^{\#}p < 0.05$ (compared to LO). The values presented were averaged from 5 measurements.

From Figure 4-30, all leave-on conditioners containing chitosan and its derivatives result in lower max loads than does the leave-on conditioner containing polyquaternium-10 (product in market). Thus, chitosan and its derivatives potentially reduce the friction during wet combing quite effectively.